Source-to-Sink Pathways of Dissolved Organic Carbon in the River-Estuary-Ocean Continuum: A Modeling Investigation

Jialing Yao[1,2], Zhi Chen[1], Jianzhong Ge[1], and Wenyan Zhang[2]

[1]State Key Laboratory of Estuarine and Coastal Research, East China Normal University, Shanghai, China
[2]Institute of Coastal Systems-Analysis and Modeling, Helmholtz-Zentrum Hereon, Geesthacht, Germany

Correspondence to: Jianzhong Ge (jzge@sklec.ecnu.edu.cn), Wenyan Zhang (wenyan.zhang@hereon.de)

Abstract. Transport and cycling of dissolved organic carbon (DOC) are most active in estuaries. However, a comprehensive understanding of the sources, sinks, and transformation processes of DOC throughout the river-estuary-ocean continuum is yet to be derived. Taking the Changjiang Estuary and adjacent shelf sea as a case study area, this study applies a physics-biogeochemistry coupled model to investigate DOC cycling the river-estuary-ocean continuum. DOC is classified into two types depending on the origin, namely terrigenous DOC (tDOC) and marine DOC (mDOC). Simulation results were compared with observation and showed a satisfactory model performance. Our study indicates that in summer, the distribution of DOC in the Changjiang Estuary is driven by both hydrodynamics and biogeochemical processes, while in winter, it is primarily driven by hydrodynamics. The spatial transition from terrigenous-dominated DOC to marine-dominated DOC occurs mainly across the contour line of a salinity of 20 PSU. Additionally, the source-sink patterns in summer and winter are significantly different, and the gradient changes in chlorophyll-a indicate the transition between sources and sinks of DOC. A five-year averaged budget analysis of the model results indicates that the Changjiang Estuary has the capability to export DOC, with tDOC contributing 31% and mDOC accounting for 69%. The larger proportion of mDOC is primarily attributed to local biogeochemical processes. The model offers a novel perspective on the distribution of DOC in the Changjiang Estuary and holds potential for its application in future organic carbon cycling of other estuaries.

1 Introduction

Dissolved organic carbon (DOC), as the largest pool of reduced carbon in the oceans (Hansell et al., 2009), is transported from rivers to oceans in the amount of approximately 0.25 Gt each year (Bauer and Bianchi, 2011). DOC is typically defined as the fraction of organic carbon ~~nonliving organic matter~~ in the ocean that can pass a ~~0.2μm~~ pore size filter ranging from 0.2-0.77μm, with decomposition time scales varying from hours to years (Asmala et al., 2014; Carlson and Hansell, 2015; He et al., 2016).

Estuaries serve as a key interface between the land and ocean, typically displaying pronounced gradients in biogeochemical variables, such as salinity, turbidity, and organic carbon (Bauer et al., 2013; Ma et al., 2023; Zhang et al., 2021). DOC in estuaries is predominantly derived from river inputs and marine in situ production~~DOC in estuaries is predominantly derived~~

30 ~~from river inputs and marine production~~ (Hu et al., 2020; Benner and Opsahl, 2001). Terrigenous DOC (tDOC), which originates from terrestrial sources (e.g., soils) and is delivered from rivers, is relatively susceptible to photodegradation but resistant to microbial degradation (Helms et al., 2008), while marine DOC (mDOC)~~, which is~~ derived _from_ fresh marine plankton production~~mainly from local production~~, tends to be consumed biochemically (Guo et al., 2021; Fellman et al., 2010). DOC of both origins can be transformed through complicated biogeochemical processes, including being converted

35 into particulate organic carbon (POC) through heterotrophy and flocculation or into dissolved inorganic carbon (DIC) through respiration (Bauer et al., 2013; Medeiros et al., 2015b). Therefore, DOC in estuaries is vital in the coastal biogeochemical carbon cycle and marine ecosystem (Meng et al., 2022; Tian et al., 2021; Herrmann et al., 2015).

Estuarine hydrodynamic environment, including the river runoff, tides, and estuarine turbidity maximum region, can significantly influence the distribution of DOC and corresponding biogeochemical processes (Li et al., 2015; Osterholz et al.,

40 2016; Le and Hu, 2013). In recent years, increasing attention has been paid to understanding the distribution and transformation of DOC in estuaries. Increased concentrations of DOC have been observed in freshwater river plumes in several estuaries, which are attributed to elevated primary production and low microbial decomposition (Marcinek et al., 2020). Production of DOC in estuaries is promoted in summer by the exudation of surface phytoplankton and the dissolution of POC from deeper regions in the water column (Druon et al., 2010). DOC concentration is significantly higher inside

45 estuaries than outside (Ji et al., 2021; Guo et al., 2021; Benner and Opsahl, 2001). However, how DOC is retained in estuaries and how much DOC from estuaries is exported to open shelf seas remain unclear. In some estuaries (e.g., the Pearl River estuary), existing studies showed that a significant portion of DOC is exported to shelf area; a unitary alteration in terrestrial DOC input results in an approximate 0.92-unit response in carbon export flux, whilst studies from other estuaries indicated that exported DOC is removed in a short time near the estuary mouth (Guo et al., 2021). A conceptual model

50 considering the turnover of DOC in estuary suggested that ~5% tDOC may be exported to the open ocean at a global scale (Anderson et al., 2019). Quantifying the contributions and impacts of individual processes for source-to-sink pathways of DOC in estuaries is challenging, and deserves focused attention and analysis (Kumar et al., 2022; Zhao et al., 2023; Sun et al., 2022; Martineac et al., 2021).

The Changjiang River is the world's fifth-largest river in terms of discharge (8.98~~9.24~~$\times10^{11}$ m^3 year^{-1}) (Zhang et al., 2022;

55 Yang et al., 2015). Its estuary (Changjiang Estuary) receives large amounts of freshwater and nutrients every year (Gu et al., 2012). It has been estimated that the Changjiang River delivers approximately 1.5~1.9 Tg DOC to the East China Sea (Wang et al., 2012; Shi et al., 2016). Besides, because of a high sediment discharge and interaction between river runoff and tides, a prominent and persistent turbidity maximum zone exists in the estuary (Ge et al., 2015; Sokoletsky et al., 2014). In this highly dynamic estuary, ~~intense anthropogenic activities,~~ terrigenous input, and the functioning of the coastal ecosystem

60 jointly control the cycling of DOC. Existing observations show that DOC concentration in the Changjiang Estuary is lower in winter than in summer, probably due to higher primary production and elevated input of tDOC through the river runoff (Ji et al., 2021). On the other hand, DOC is removed rapidly in this area due to intense photooxidation and microbial degradation (Guo et al., 2021). Due to the diverse sources and pathways associated with DOC, a more specific exploration is

2

needed to understand the source, sink, and transportation through Changjiang Estuary within the context of physical and biogeochemical processes at the estuary.

This study combines field observations and high-resolution numerical modeling to investigate the source-to-sink pathways and transformation of DOC in the Changjiang Estuary by distinguishing tDOC and mDOC. In order to derive a process-based understanding of the DOC cycling in the river-estuary-ocean continuum, we quantified the impacts of relevant biogeochemical processes, ~~analyzed~~analysed key hydrodynamic and biogeochemical factors, and estimated the transport fluxes across different compartments from the estuary to the open ocean.

2 Methods and Data

2.1 Model description

A three-dimensional hydrodynamic model coupled with a biogeochemical model is applied in this study. The physical model is the unstructured grid, Finite-Volume Community Ocean Model (FVCOM) (Chen et al., 2003), providing simulations of physical properties and hydrodynamic processes in the study area. The finite volume method and use of an unstructured grid in FVCOM facilitate the handling of intricate geographic boundaries as estuaries and islands with irregular shorelines (Chen et al., 2013). An integrated model, FVCOM-SWAVE, was incorporated into FVCOM for the simulation of waves and wave-current interactions (Qi et al., 2009). Besides, FVCOM encompasses a sediment transport model to simulate sediment and suspended particulate matter (SPM) dynamics (Ge et al., 2015). A complete coupling of current-wave-sediment interactions is implemented in FVCOM (Wu et al., 2011; Ge et al., 2018; Ge et al., 2020).

The European Regional Seas Ecosystem Model (ERSEM) is a biogeochemical and ecological model for complex ecosystems in both pelagic and benthic environments of regional seas (Butenschön et al., 2016). It offers a platform for simulating the microbial food web and major biogeochemical cycles, including carbon, nitrogen, phosphorus, silicate, iron cycling, calcification, and a light model based on inherent optical properties. We used the Framework for Aquatic Biogeochemical Models (FABM) (Bruggeman and Bolding, 2014) as a coupler for data exchange between the hydrodynamic model (FVCOM) and the biogeochemical model (ERSEM).

2.2 DOC cycle module

The DOC cycle module in the coupled FVCOM-ERSEM model distinguishes terrigenous and marine components in the river-estuary-shelf continuum (Anderson et al., 2019). A schematic of the DOC module is shown in Fig. 1.

DOC represents the carbon fraction within dissolved organic matter (DOM) (Hopkinson and Vallino, 2005). As for terrigenous components, terrigenous ~~dissolved organic matter (~~DOM~~)~~ contains a significant portion of aromatic compounds (Verhoeven and Liefveld, 1997), which tends to be photo-oxidized while resistant to decomposition by microorganisms (Opsahl and Benner, 1998; Hudson et al., 2007). ~~Moreover, aromatic compounds are precipitated as a result of metal ions (Vilge-Ritter et al., 1999).~~ Therefore, based on the unified DOM model (UniDOM) (Anderson et al., 2019), tDOC is divided

3

95   into photolabile (T_1) and non-photolabile (T_2) pools. T_1 undergoes photodegradation and flocculation but is not prone to microbial decomposition, while T_2 does not undergo photodegradation and flocculation but is prone to microbial decomposition. Both T_1 and T_2 are further divided into three components to take into account the decrease of turnover rate over time (Table S1). The three components represent turnover time scales of 30 days, 8 years, and 70 years, respectively, following existing reference studies (Catalán et al., 2016; Evans et al., 2017; Anderson et al., 2019). T_1 comprises T1_30d,

100   T1_8y, and T1_70y, while T_2 comprises T2_30d, T2_8y, and T2_70y. In the model, tDOC cycling is affected by three biogeochemical and physical processes, namely (1) photolysis, (2) bacterial uptake, and (3) flocculation. In the marine components, mDOC is categorized into three pools (R_1, R_2, and R_3) derived from the dynamic decomposition model in ERSEM, ~~labeled~~labelled explicitly as labile, semi-labile, and semi-refractory mDOC. This classification is determined by considering degradation timescales and production mechanisms. Based on the nomenclature by Hansell (2013), the existing

105   biological model does not account for the century-scale lifespan of refractory DOC (Butenschön et al., 2016; Polimene et al., 2007). Given that our simulation period ranges for five years, this simplification is considered reasonable. mDOC primarily originates from the mortality and excretion of bacteria, as well as the excretion and mortality of phytoplankton and zooplankton. It is subsequently consumed through bacterial uptake. In the model, mDOC cycling is influenced by six biogeochemical processes, namely (1) phytoplankton mortality, (2) phytoplankton excretion, (3) zooplankton mortality, (4)

110   zooplankton excretion, (5) bacterial uptake, and (6) bacterial excretion. A detailed description and equations of the cycling and associated parameterizations are given in Text S1 from the Supplementary Information.
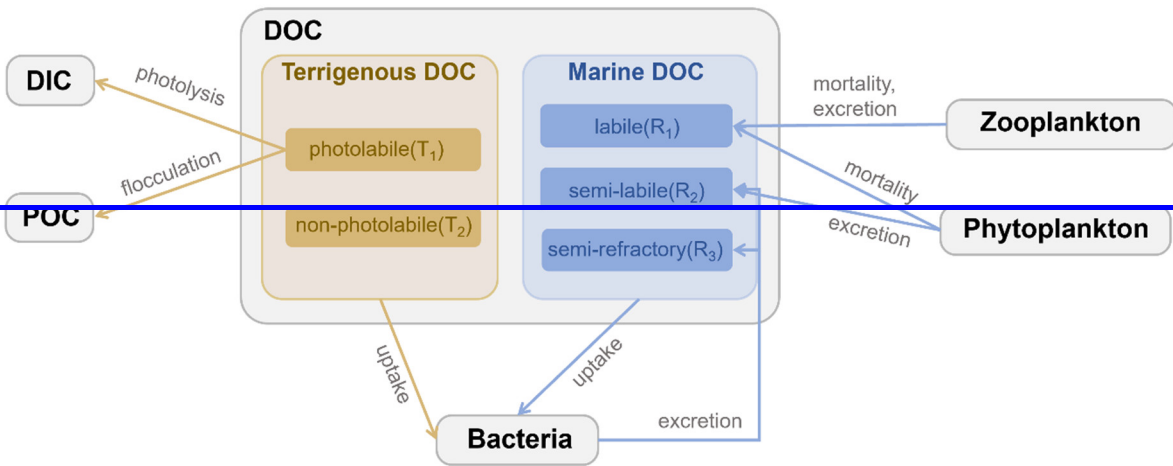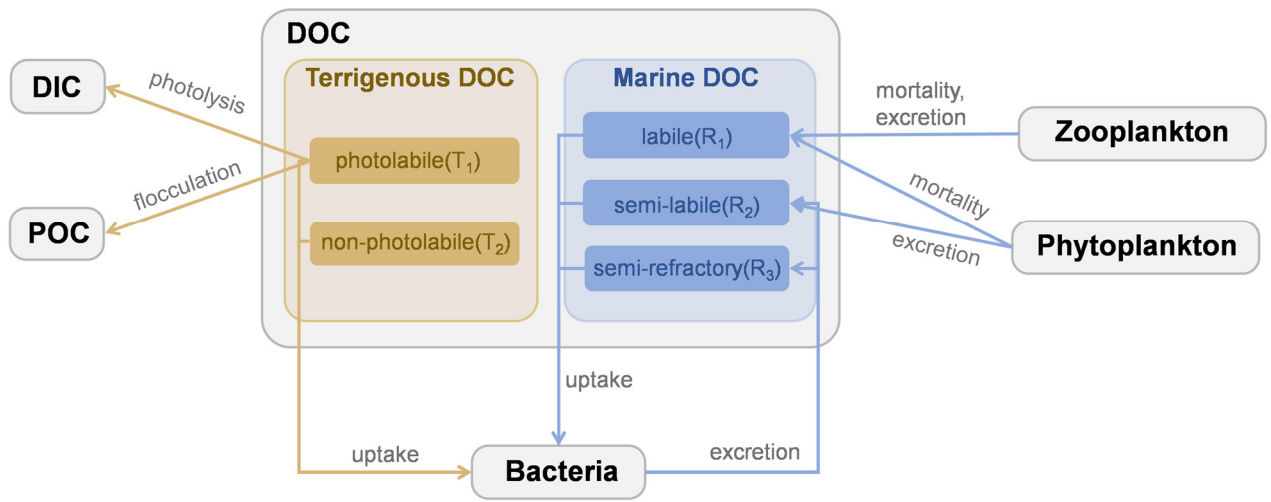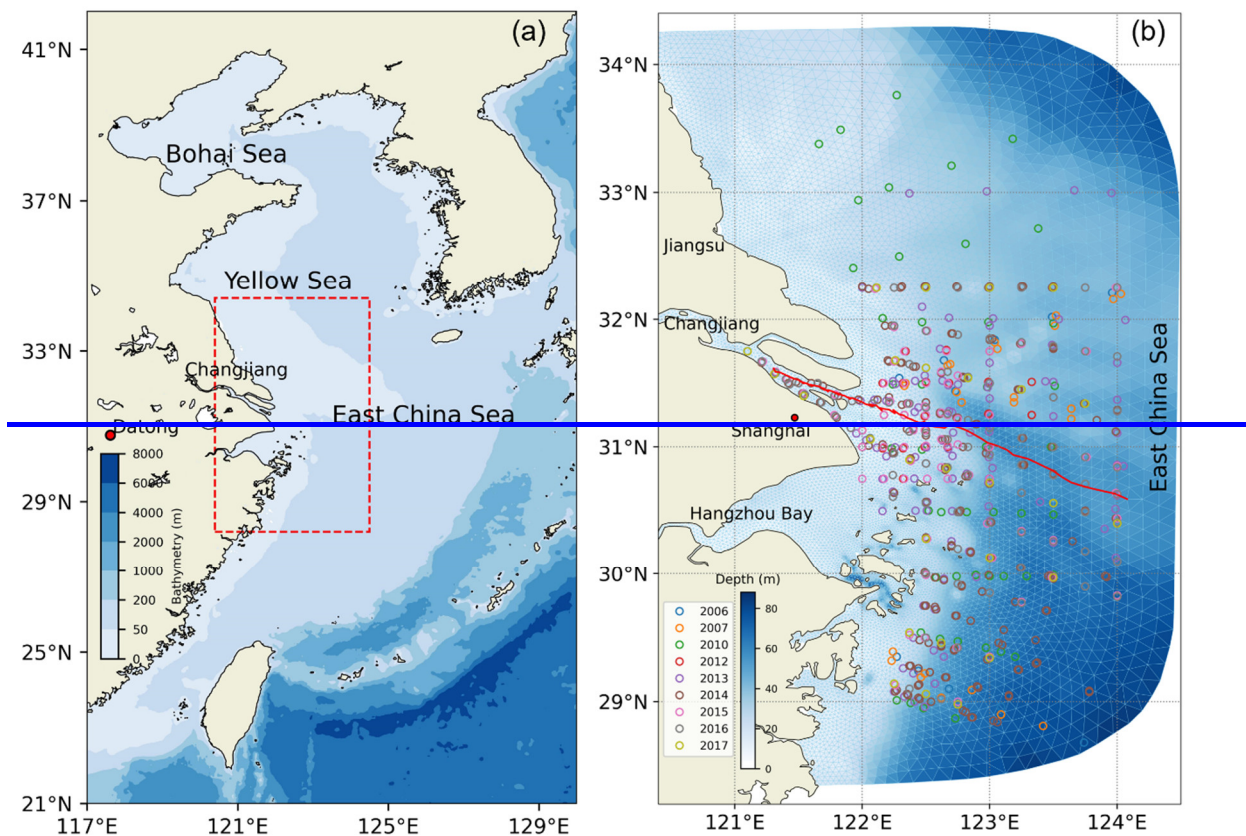
Figure 1. The flow diagram presents the sink and source terms of DOC.

2.3 Model setup for the study area

The model domain for the Changjiang Estuary (Fig. 2) extends from the Datong hydrological station as the upstream boundary in the Changjiang River to the inner shelf of the East China Sea (ECS).
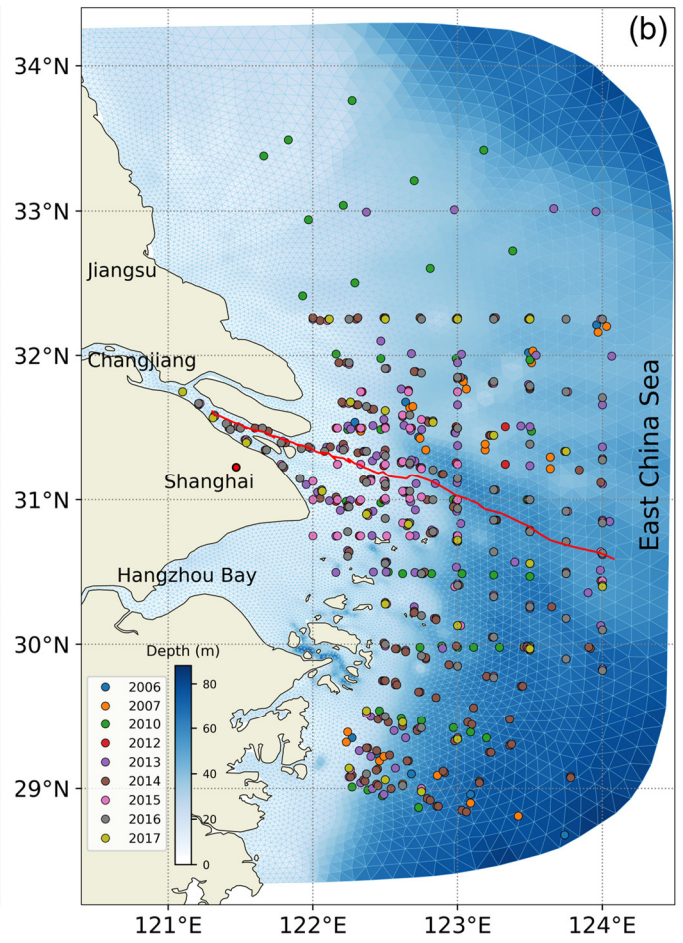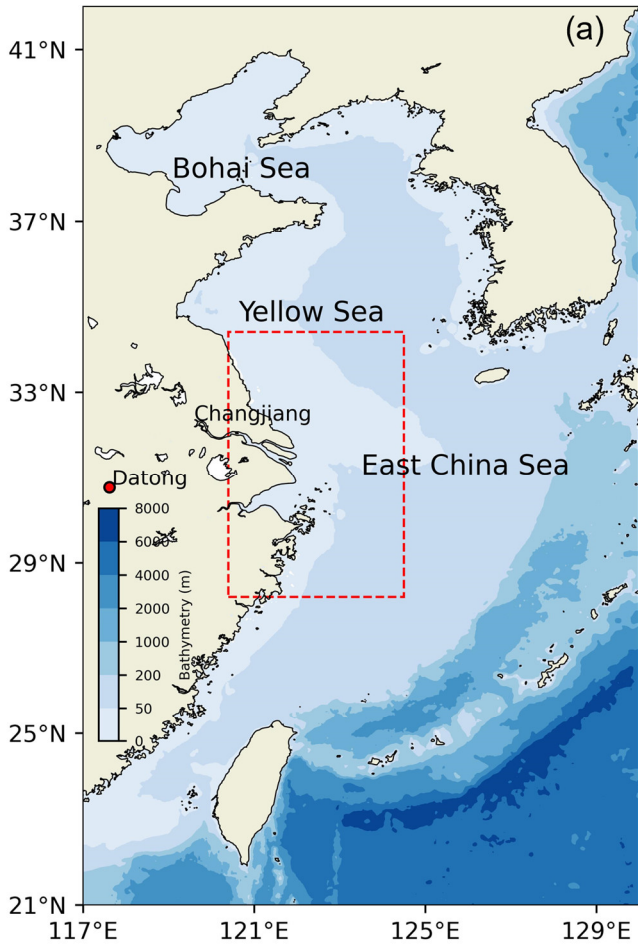
Figure 2. Map of the study area. The panel (**a**) shows the location of the Changjiang Estuary, with the red rectangle indicating the study area. The panel (**b**) presents the model domain resolved by a triangular grid. The circles mark the sampling locations of DOC concentration between 2006 and 2017, distinguished by different ~~colored~~coloured circles. The red solid line is the selected transect from the river channel to the open shelf region for analysis.

The spatial resolution of the model grid is between 1 and 3 km near the river mouth, and between 4 and 15 km at the open boundary. The upstream river boundary at the Datong station is forced by the daily recorded freshwater discharge and SPM flux. Meanwhile, nutrient concentrations, tDOC, and POC concentrations are specified at the river boundary. The organic carbon concentrations based on the climatological average concentration at the river boundary for reference are derived from field observations conducted by multiple origins (Shi et al., 2016; Guo et al., 2014; Wang et al., 2012; Zhang et al., 2014; Liu et al., 2013; Liu et al., 2019). Open boundary conditions are derived from a shelf-scale FVCOM extended to the East China Sea (ECS) to provide astronomical tides and ocean circulations (Ge et al., 2013; Ge et al., 2020). Atmospheric forcing is derived from the global climate and weather reanalysis hourly dataset ERA5 produced by the European Centre for Medium-Range Weather Forecasts (ECMWF). This includes the 10-meter surface wind speed, long waves, short waves, and sensible and latent radiation flux at a spatial resolution of 0.125°. The atmospheric partial pressure of CO_2 (pCO2) is set to a constant value of 385 ppm. The sea surface temperature was assimilated using high-resolution satellite data from GHRSST/JPL (https://podaac.jpl.nasa.gov/GHRSST), with a spatial resolution of 0.011°. Waves and sediment dynamics

7

were incorporated into the model (Ge et al., 2013). The model simulation covers a five-year period from 2013 to 2017, with a computational time step of 6 s.

A key configuration of parameters associated with DOC cycling in the coupled ERSEM model could be referred to Table S1 in the supplementary information. After undergoing univariate verification (chlorophyll-a) and multivariate verification through the application of principal component analysis (involving factors such as temperature, salinity, sediment, and nutrients) in the Changjiang Estuary, this coupled model FVCOM-ERSEM was utilized within the framework developed by Ge et al. (2020) for further simulation and analysis of DOC.

2.4 ~~Model setup for the study area~~Data compilation and synthesis

To enhance our understanding of DOC cycling in the Changjiang Estuary, we have compiled and synthesized historical data of DOC concentration based on observations. The procedure included data retrieval, extraction of image-based data, data cleaning (involving the removal of duplicate and outlier values, exclusion of data outside the research area, and standardization of data units), as well as data visualization. The sites of DOC observation are shown in Fig. 2. A compilation of all data sources is listed in Table 1. In this compiled dataset, 869 data points are for the surface water, and 757 data points are for the bottom water which corresponds to a location 2-5 meters above the local seabed. The dataset encompasses observation in all four seasons from the period of 2006 - 2017 in the region stretching from the south branch of the Changjiang Estuary to the adjacent coastal area.

Table 1. The reference sources of historical DOC concentration data.

Time	Surface Number	Bottom Number	Data Source
July 2006	12	-	Shi et al. (2013)
January 2007	12	12	Shang et al. (2012)
November 2007	12	12	Zhang et al. (2011)
May 2010	47	36	Zhang et al. (2013)
February 2012	21	21	
May 2012	21	21	
August 2012	22	22	Xing et al. (2014)
November 2012	22	22	
March 2013	85	85	Wang et al. (2014); Gao et al. (2020)

August 2013	28	30	Yuan et al. (2015)
February 2014	106	106	Gao et al. (2020)
May 2014	7	-	Guo et al. (2018)
July 2014	100	104	Gao et al. (2020)
October 2014	8	-	Guo et al. (2018)
July 2015	94	18	Gao et al. (2020)
November 2015	26	26	Zhang et al. (2018)
March 2016	89	89	Gao et al. (2020)
July 2016	87	84	
February 2017	26	26	
May 2017	27	26	Guo et al. (2021)
July 2017	17	17	

3 Results

3.1 Model validation

155 The FVCOM-ERSEM coupled model has been proven to reproduce the distribution of chlorophyll-a, nutrients, and suspended sediment concentration in the Changjiang Estuary effectively (Ge et al., 2020). In this study, we assess the model performance in the DOC concentration. Based on the compiled observational dataset, a comparison was conducted between the model results and the observation data (Fig. 3). Because the observational data include only monthly records, a point-to-point comparison was performed using model monthly-averaged data corresponding to the respective time periods, covering

160 the simulation time from 2013 to 2017. The scatter plots (Fig. 3a, b) show a general agreement between the model results and observations with root mean square deviation (RMSD) of 282 and 249 mg m^{-3} in the surface and bottom water, respectively, and the normalized RMSD is 0.25 for both layers. The statistical results of the DOC concentration comparison are displayed in the Taylor diagram (Fig. 3c), which shows that the ~~centered~~centred RMSD for both the surface and bottom water is below 250 mg m^{-3}, with the standard deviation (SD) remaining around 300 mg m^{-3}. The correlation coefficient (CC)

165 is close to 0.7. In addition, the spatial distribution of simulated DOC also shows a similar range with the observation data at a seasonal scale (Fig. S1 in the Supplementary Information). Based on these overall good agreements with observation data, the model proves to be capable of capturing the distribution and variation of DOC in the Changjiang Estuary.

9
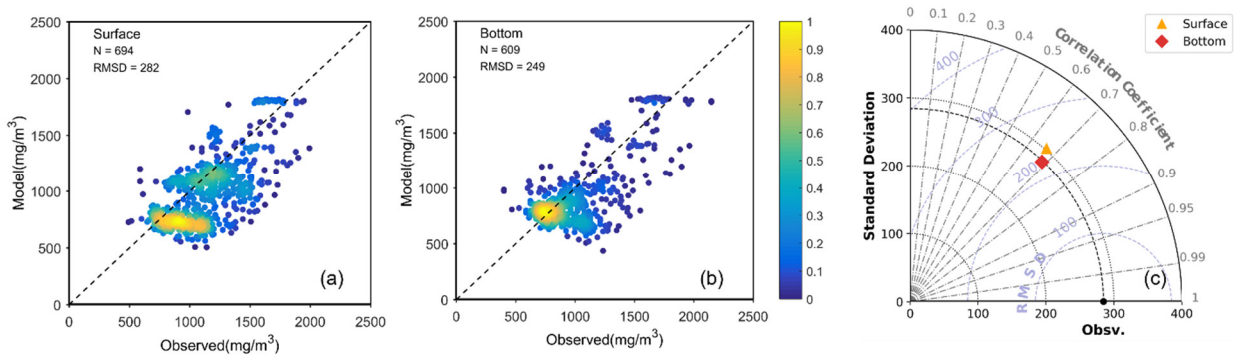
Figure 3. Model comparison with observational data for the period from 2013 to 2017 in the surface and bottom water, respectively. (**a**) and (**b**) represent scatterplot density maps of the model-observation comparison for the surface and bottom water, respectively. Color denotes the density of data points. (**c**) depicts the Taylor diagram, with the orange triangle representing the data in the surface water and the red diamond representing the data in the bottom water.

3.2 Distribution of DOC and its components tDOC and mDOC

To figure out the seasonal distribution characteristics of DOC, the seasonal average of the model results over the years 2013-2017 was calculated for all four seasons. Results indicate two distinct seasonal patterns in summer and winter (Fig. 4).

Spatially, there is a declining trend in DOC concentrations from the river to the offshore region. Maximum DOC concentrations are typically found close to the river channel. In general, DOC concentration in the summer season is higher than in the winter season and exhibits a more extensive distribution of high concentration values (> 1400 mg m^{-3}). This phenomenon is attributed to the increased summer runoff and prevailing southerly winds. In winter, driven by the northerly winds, the freshwater plume shifts southward, with a subsequent southward shift of DOC distribution. Meanwhile, because of reduced river runoff and strengthened tidal effects, the dispersion range of DOC is constrained. Furthermore, in summer, there is a ~~significant contrast~~more distinct difference of DOC between the surface and bottom layer, while during the winter, the vertical differences are relatively minor. In the contour maps of DOC and salinity distribution, the nearshore DOC distribution closely resembles the salinity distribution, highlighting that physical mixing predominantly governs the distribution of DOC at the estuary. However, during the summer, at the boundary of transition between plume and saltwater (Salinity=31), the distribution of DOC shows no significant correlation with salinity, whereas, in winter, their distributions exhibit a higher consistency.
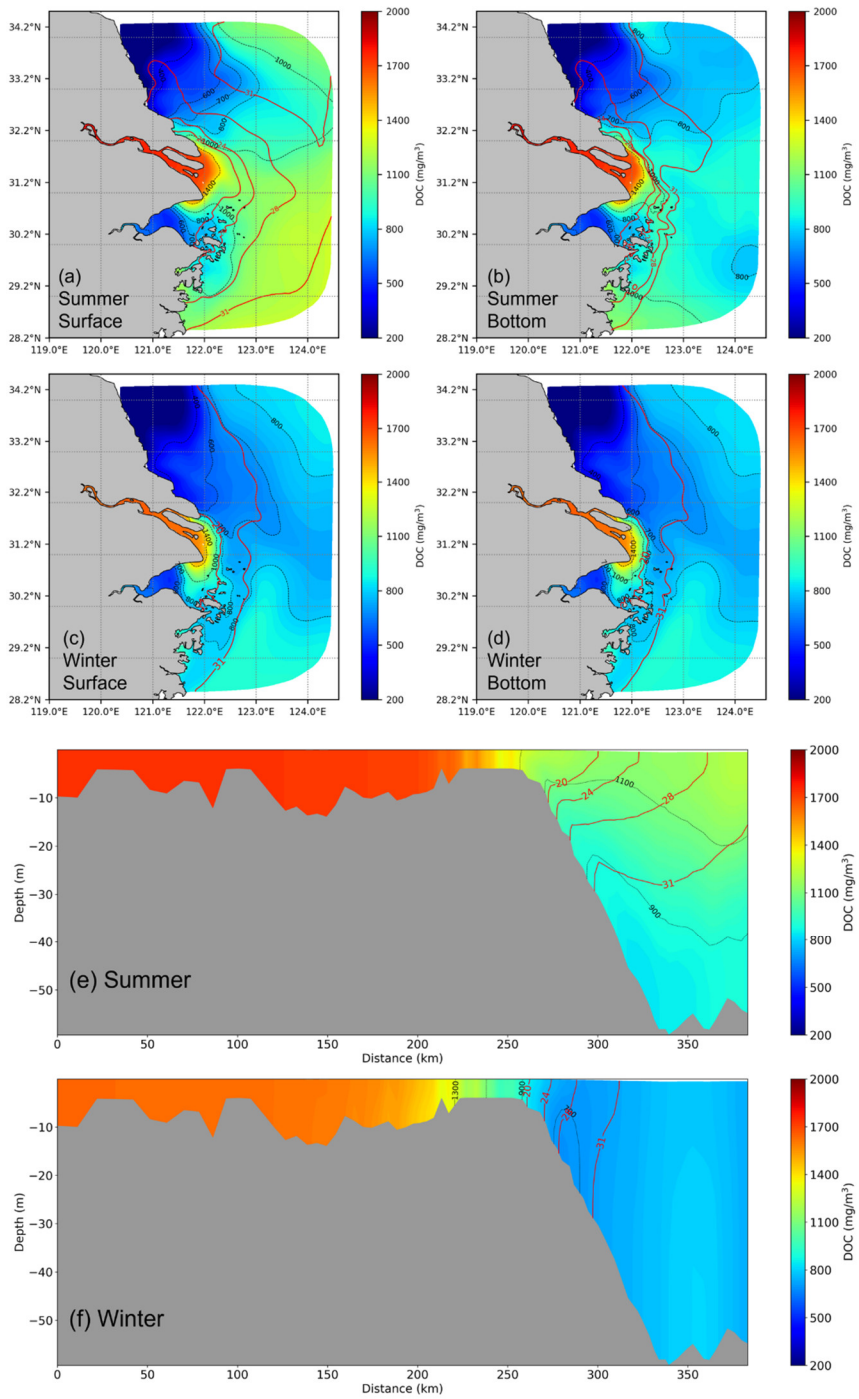
10

Figure 4. DOC spatial distribution from model is based on a five-year average for both surface and bottom layers (a-d) and vertical distribution (e, f) in summer and winter along the selected transect from river to shelf. The red contour lines represent salinity, while the black contour lines indicate DOC concentration.

11

Spatial distribution of DOC concentration along the pre-defined transect (Fig. 2) provides more details of the change from the estuary towards the offshore region (Fig. 4e-f). In summer, a notable stratification exists in the region where salinity exceeds 20 PSU along the transect. The vertical distribution of DOC is highly similar to the salinity contour within low- and mid-salinity (salinity<20) regions, showing aligning with conservative mixing with salinity, while the inconsistent distribution of DOC in higher salinity may be attributed to the dominance of other signals, such as local biogeochemical process in deep region. In winter, enhanced mixing due to surface cooling leads to a nearly homogeneous DOC concentration in the water column with little vertical gradient. These distribution characteristics suggest that in summer, the distribution patterns of DOC in the low- and mid-salinity area are dominated by physical hydrodynamics, while in the offshore area, there are other factors influencing the distribution of DOC. In winter, it is primarily driven by hydrodynamic factors.

The total DOC concentration is divided into tDOC and mDOC for analysis of the origin. The proportion of tDOC shown in Fig. 5 shows that the isoline of 0.5, which indicates that the proportion of tDOC and mDOC is equal, is located quite close to the contour line of salinity of 20 PSU in both summer and winter seasons. It can be seen that the distribution of tDOC is largely constrained by the transport of diluted water. The extension of tDOC is broader, and differences between the surface and bottom layers are more pronounced in summer than in winter.
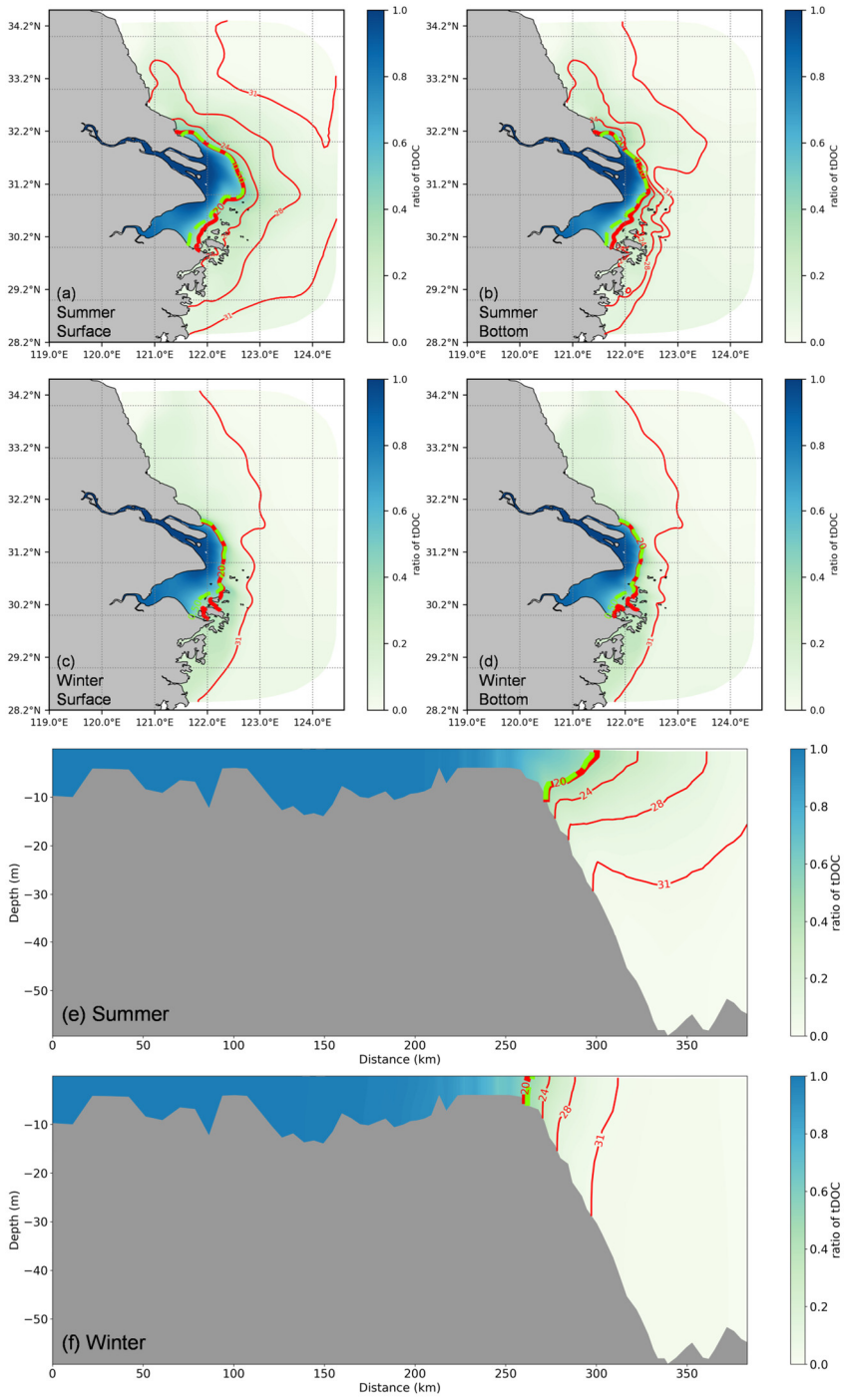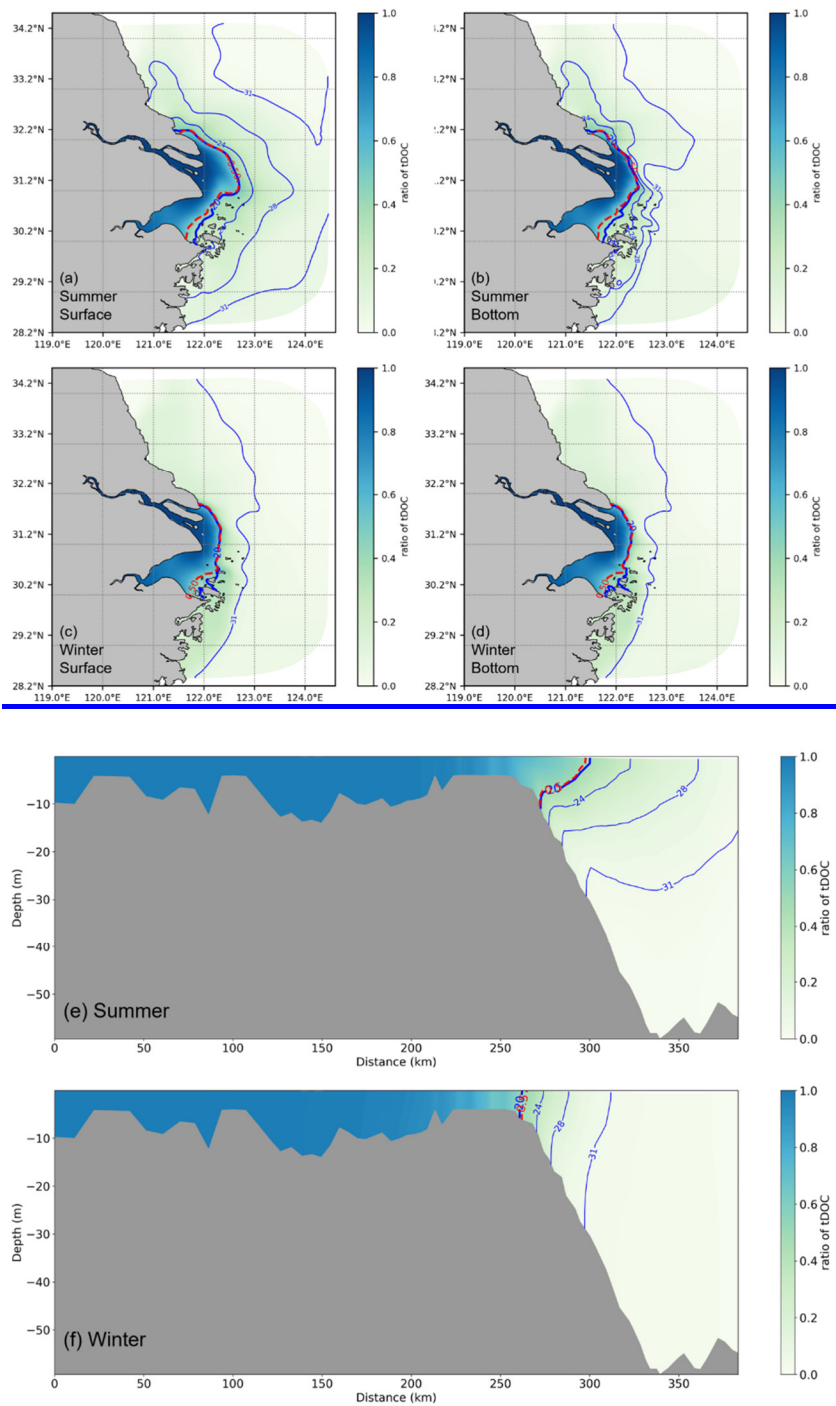
Figure 5. The proportion of tDOC in total DOC is calculated based on a five-year average in summer and winter. The proportion of horizontal distribution for both surface and bottom layers and vertical distribution in summer and winter. The blue contour lines represent salinity, with the red contour lines indicating a ratio of 0.5.

3.3 Time series variation of DOC in the estuary

To further figure out the driving mechanisms for the distribution of DOC and its components, the study area is divided into four sub-regions (Fig. 6a, b) based on the distribution of salinity, namely the river channel, the river mouth, the river plume,

215   and the open shelf. Considering the temporal variation of the river plume, delineation of the sub-regions is distinguished between wet (May to October) and dry (November to April) periods.

The time series of DOC and its components tDOC and mDOC spatially vertically averaged in each sub-region is shown in Fig. 6c-e. Concentration of the total DOC gradually decreases from the river channel to the continental shelf, and the concentration in the plume area is comparable to that in the open shelf region. The temporal variation of DOC in the river

220   channel is mainly influenced by the climatological average concentration of DOC input from the river boundary, which does not exhibit a distinct summer-high and winter-low single peak pattern. Instead, the temporal variation of the DOC from river discharge shows a generally lower level in the first five months of the year (Jan-May) compared to the following seven months (June-December) but superposed with large monthly fluctuations. Such river discharge-induced variation also significantly affects the DOC concentration in the river mouth sub-region. By contrast, the plume and open shelf region

225   exhibit pronounced summer-high and winter-low pattern with relatively smooth transition in spring and autumn. Our ~~modeled~~modelled variation of total DOC concentration is consistent with previous observational studies (Liu et al., 2014; Ji et al., 2021; Guo et al., 2021; Han et al., 2021). This variation is associated with the change of terrigenous and marine components (Fig. 6d, e). tDOC decreases gradually from the river to the open shelf region, whilst mDOC shows an opposite trend. The river channel and river mouth sub-regions are dominated by tDOC, which contributes to more than 85% of the

230   total DOC. In the plume area, the concentration of mDOC becomes larger than tDOC, suggesting a shift of dominance in the origin. The open shelf sub-region is dominated by mDOC, which takes up more than 90% of the total DOC.
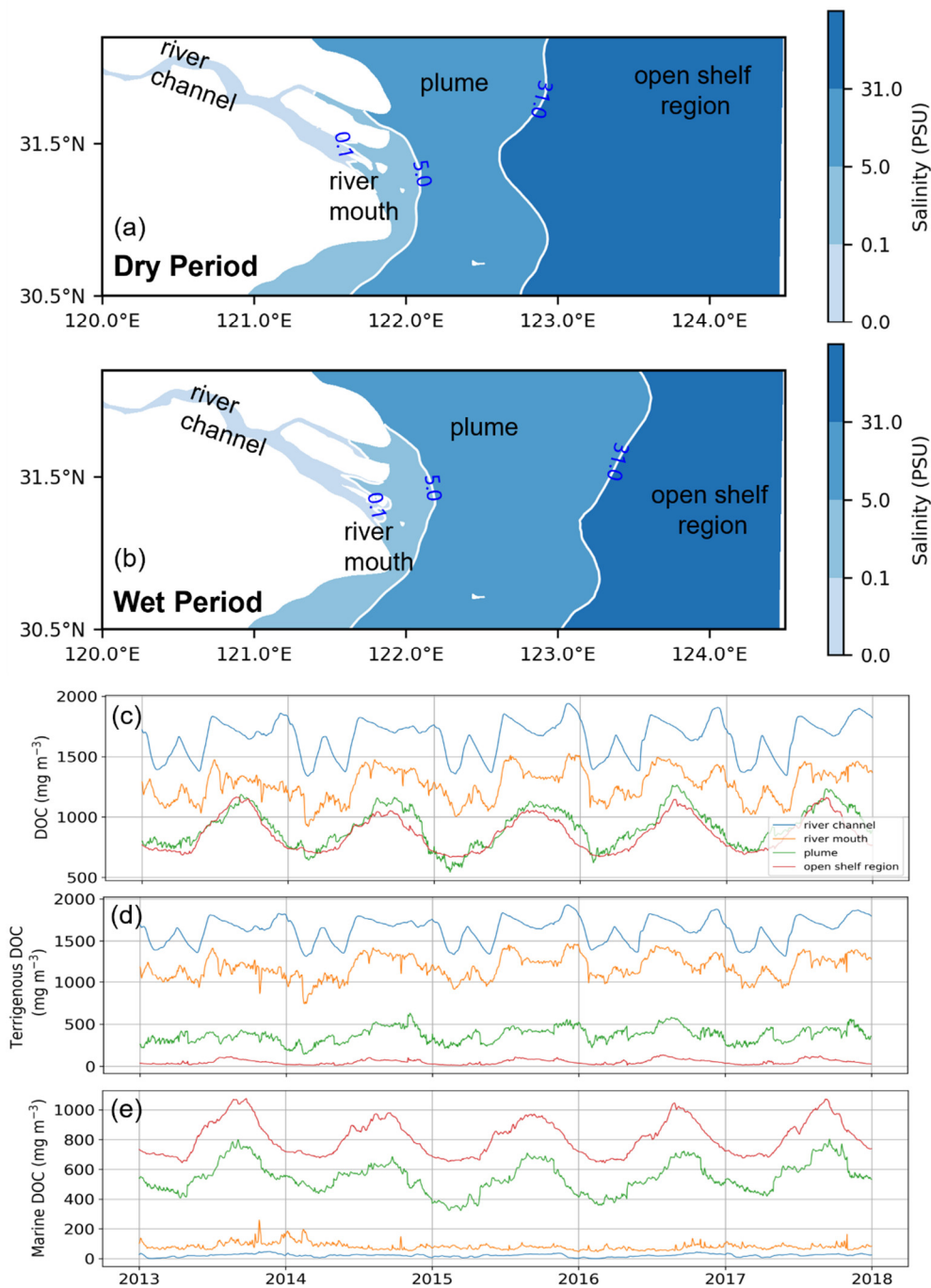
15

Figure 6. The partition of the model study area into four sub-regions based on the vertical average of salinity (**a, b**). The region with salinity less than 0.1 PSU is classified as the river channel, 0.1-5 PSU is the river mouth, 5-31 PSU is the plume, and the reminder region with salinity greater than 31 PSU is defined as an open shelf region. Time series of the concentration of total DOC (**c**) and its components tDOC (**d**) and mDOC (**e**) in the four sub-regions. Blue, orange, green, and red lines represent regions of river, river mouth, plume, and open shelf region, respectively, and all concentrations are regional vertical averages.

The distribution and cycling of DOC are intimately linked with various biogeochemical processes. The daily vertical average rate in different processes that act as source or sink of DOC is calculated respectively in the model and shown in Fig. 7. Since tDOC in the study area derives exclusively from river discharge, only sink terms of tDOC are calculated. The decreasing rate of tDOC in the sink terms from the river to the open shelf region indicates that tDOC is gradually consumed, resulting in a reduction in concentration during its transport towards the open shelf. Among the sink terms of tDOC, photolysis exhibits pronounced fluctuations, while the rate of bacterial uptake shows relatively smooth variation along the river-estuary-ocean continuum. The production (source) and consumption (sink) rates of mDOC both exhibit a gradual increase from the river to the open shelf region. mDOC production and consumption are more active from around January to July. After July, the production and consumption rates of mDOC declined rapidly and remained consistently low until the end of the year. Consequently, DOC concentration accumulates to its maximum during summer and gradually declines to its minimum in the winter (Fig. 6c). Among the production terms of mDOC, in the plume and open shelf region, phytoplankton release exhibits the highest rate, followed by zooplankton release and bacterial release in descending order (Fig. 1Fig. 1). mDOC is consumed mainly by bacteria. The bacteria uptake rate (sink) of mDOC is much higher than the bacterial production rate through release (source). The ecosystem model ERSEM includes the bacteria-mediated production of recalcitrant DOC (Hansell, 2013), which represents the most difficult-to-digest semi-refractory DOC in the model. Therefore, the newly produced mDOC from bacteria is added to the pool of semi-refractory mDOC, thereby an implementation of microbial carbon pump (Jiao and Azam, 2011; Jiao et al., 2014) The released mDOC from bacteria is converted into semi-refractory mDOC(Jiao et al., 2010; Jiao et al., 2014; Hansell, 2013). In summary, bacterial uptake is the major process for the removal of DOC (mostly tDOC) in the river channel and river mouth regions. The plume region serves as a transitional zone, where the bacterial uptake rate of tDOC decreases while the bacterial uptake rate of mDOC increases. Meanwhile, the production of mDOC by processes such as release from phytoplankton, zooplankton, and bacteria also becomes prominent in the plume region and offsets the loss of DOC. In the open shelf region, DOC (mostly mDOC) is mostly produced by phytoplankton release (source) and consumed by bacteria uptake (sink), with secondary contributions from zooplankton release and other processes.

17
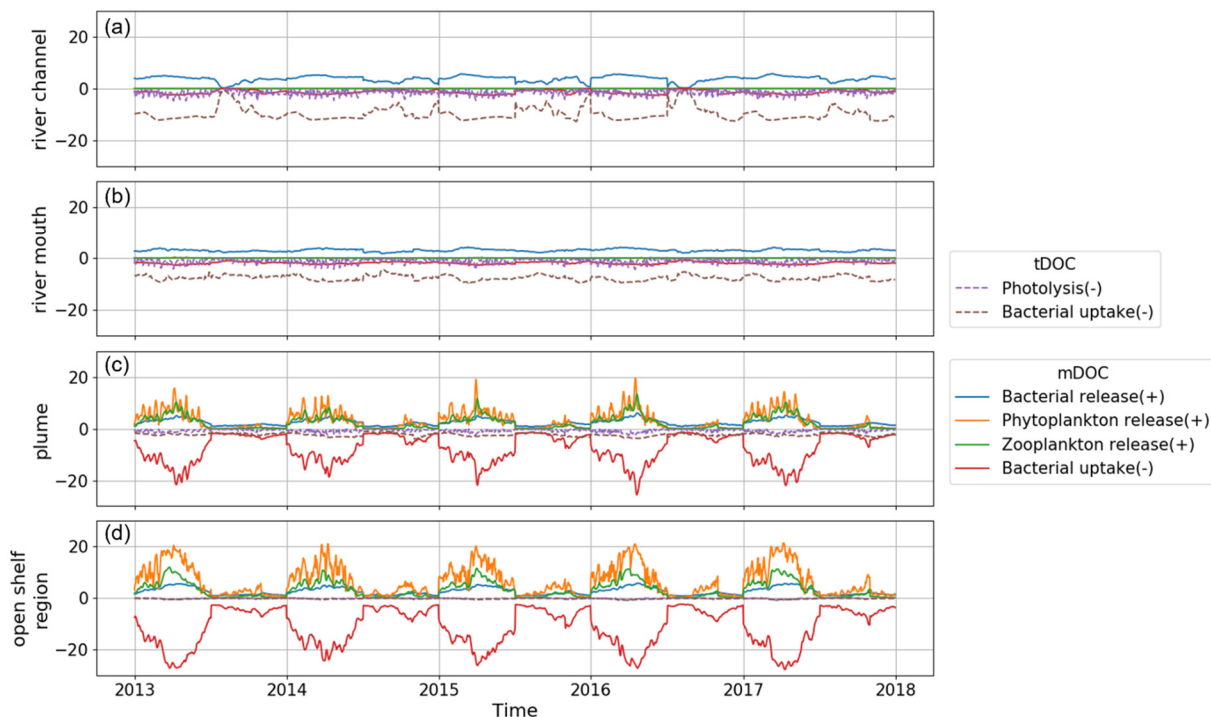
Figure 7. Daily vertical average rate (Units: mg m^{-3} d^{-1}) of production (source) and consumption (sink) of tDOC (dashed lines) and mDOC (solid lines) in the four sub-regions. Positive values indicate sources, while negative values indicate sinks.

3.4 Transformation of DOC in the River-Estuary-Ocean Continuum

After deriving a general understanding of the distribution of DOC and its components, further analysis was conducted focusing on the transformation of DOC in the source-sink dynamics. Our results show that in summer, the transition from a net sink to a net source of DOC occurs gradually through the river-estuary-ocean continuum. The crucial interface for the shift between the net sink and the net source is located at the area characterized by a significant gradient of chlorophyll-a concentration. This interface is influenced by physical mixing and aligns closely with the contours of salinity (Fig. 8a, b). As shown in Fig. 5, tDOC is gradually diluted, mixed, and consumed by biogeochemical processes (photolysis and bacteria uptake) along the river-estuary-ocean continuum, whilst the activities of plankton and bacteria gradually intensify towards the open shelf, leading to a shift from tDOC-dominated to mDOC-dominated DOC. With production rates surpassing consumption rates, DOC accumulates in summer, implying a transformation of the estuary from a sink to a source of DOC. The change in the spatial gradient of Chlorophyll-a concentration serves as a practical indicator for this transformation (Fig. 8c, d).

18

In winter, the majority part of the estuary acts as a DOC sink. During this season, with a low temperature (average around 10 ℃) and limited nutrient fluxes from the river, biological activity rates are much reduced compared to summer. The interface for the transition from sink to source is shifted offshore and to the southeast corner of the model area.
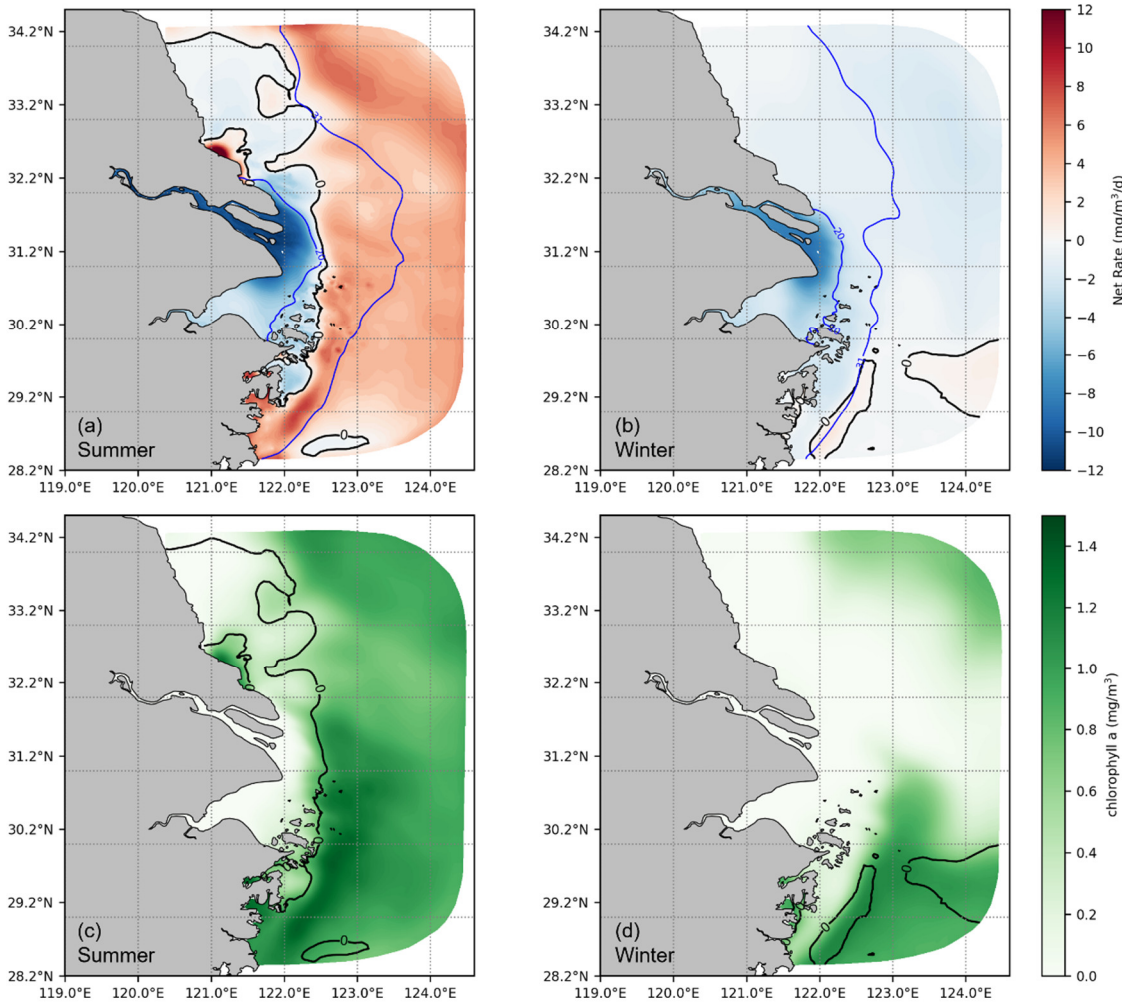

Figure 8. Vertical average net cycling rate of DOC (**a, b**) and chlorophyll-a (**c, d**). The solid black line indicates a net cycling rate at zero, and the solid blue line represents the vertical average salinity (units: PSU).

Along the transect, starting from the river channel to the shelf, vertical averaged production and consumption rate of DOC by each relevant process is calculated (Fig. 9). The result shows that in summer, among the production terms, the rate related to bacteria is relatively stable along the transect. Production by both phytoplankton and zooplankton starts to increase where salinity exceeds 5 PSU and continues until 30 PSU, where the growth of chlorophyll-a concentration is relatively stable. Among the consumption terms, the rates of various processes exhibit minimal changes in the river channel and river mouth regions. Upon entering the plume area, the rates of bacterial activity and photolysis of tDOC exhibit a decreasing trend.

19

Simultaneously, the bacterial consumption rate of mDOC gradually rises, assuming a dominant role before stabilizing. With regard to the change in the net rate (indicated by the solid black line in Fig. 9), the largest gradient is seen in the plume area, marked by a transition from negative values (sink) to positive values (source), and becomes smooth. This indicates a rapid and complex biogeochemical transformation of DOC in the estuary. In winter, the rates of all processes are reduced compared to summer, remaining the significant rate transitions in the plume area. Compared to the summer season, planktonic organism rates reach their peak in the open shelf region, where chlorophyll-a concentration is maximal. The total consumption rate slightly exceeds the total production rate, resulting in an overall negative net rate along the entire transect.
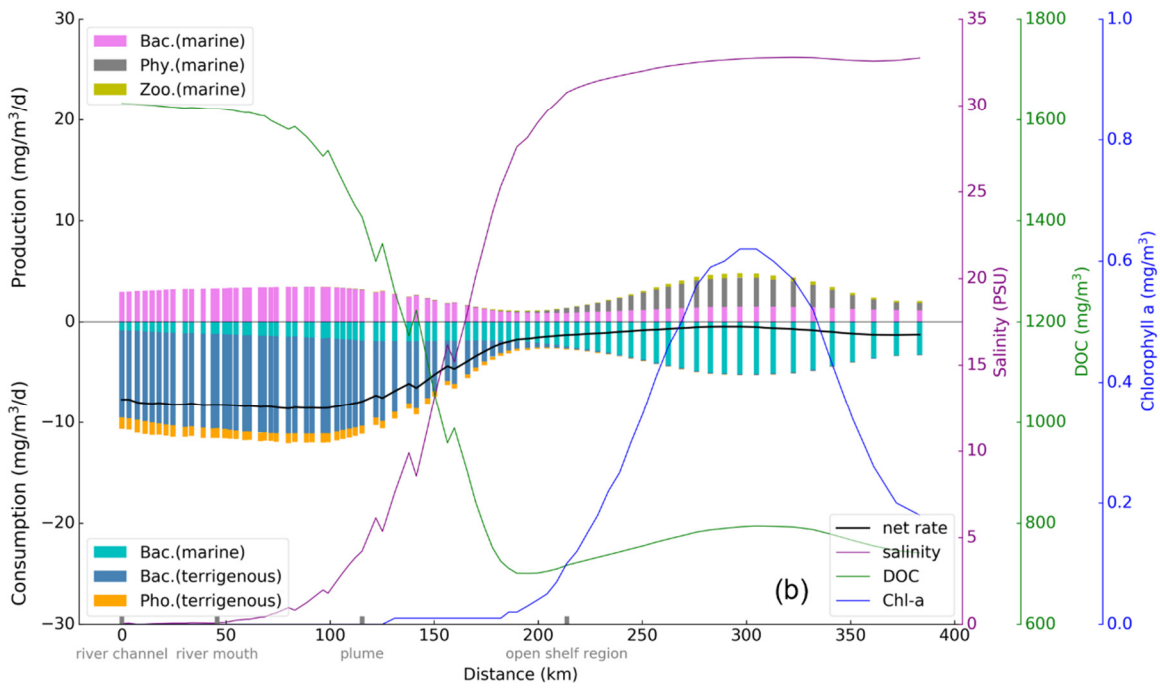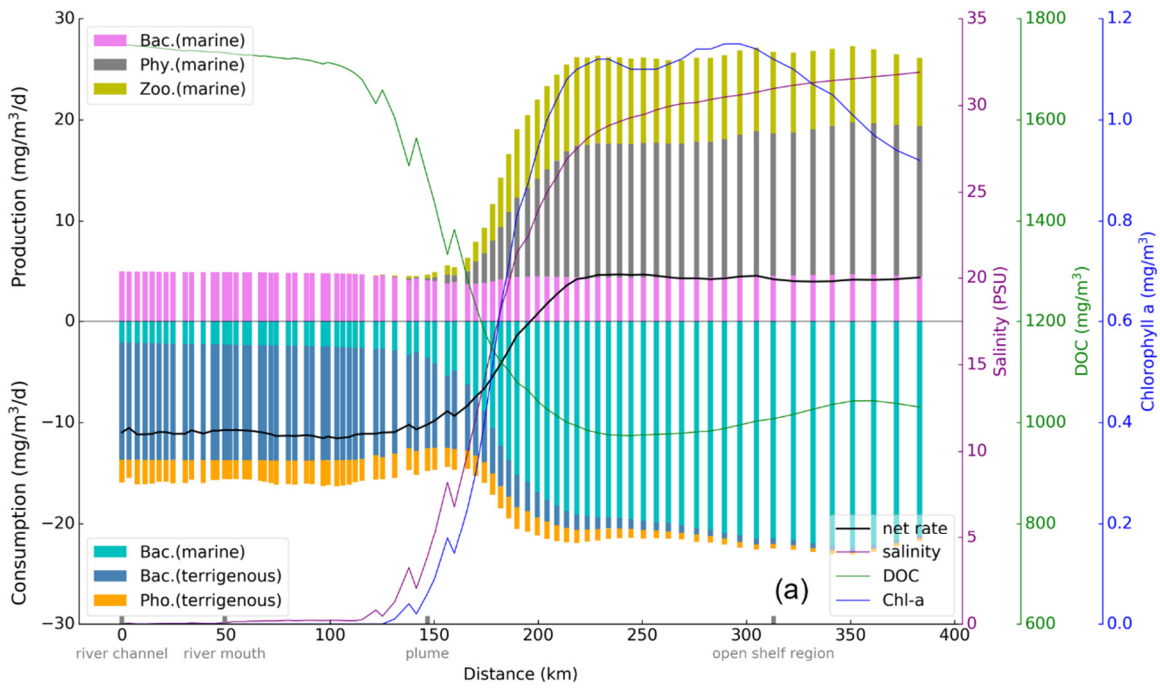
Figure 9. Vertical average production and consumption rates of DOC along the transect from the river channel to the shelf in summer (**a**) and winter (**b**).

3.5 Budget analysis

300   To further identify the role of the Changjiang Estuary in the source-to-sink pathways of DOC, budget analysis was carried out for the whole model domain. In this study, budget analysis was based on the annual average over the five years (2013-2017). Input and output of DOC at the boundary, as well as production and consumption terms within the model domain, were taken into account. Results shown in Table 2 indicate that the Changjiang Estuary received 1.53±0.13 Tg/yr of DOC from the river, which is consistent with previous studies (Shi et al., 2016; Wang et al., 2012). The export of DOC to adjacent

305   open ocean is 2.26±0.22 Tg/yr, greater than the input value. It should be noted that the export of mDOC refers to the net export (output – input). Therefore, the import of mDOC is indicated as 0. This result indicates that the Changjiang Estuary as a ~~whole acts~~whole act as a source of DOC. This is partly due to a larger production (28.91±1.07 Tg/yr), which exceeds the consumption (28.52±1.03 Tg/yr) of mDOC in the model domain, and partly due to the export of unconsumed tDOC from the upstream river. In the exported DOC, tDOC accounts for 0.69±0.08 Tg/yr (equivalent to ~31% of the total export), while

310   mDOC contributes 1.57±0.18 Tg/yr. Since there is no local production of tDOC in the model domain, the ratio of the exported tDOC to the imported tDOC indicates that ~55% of imported tDOC from the upstream river is consumed within the Changjiang Estuary (by photolysis and bacterial uptake), and the rest 45% is exported to the open ocean. By contrast, mDOC is mostly (~96%) recycled within the model domain, despite that it accounts for a major portion (~69%) of the exported DOC.

315   **Table 2.** Budgets of annual mean input, output, and internal production and consumption of DOC with standard deviations in the Changjiang Estuary (units: Tg/yr, $1Tg=10^{12}g$).

Component	Import	Export	Production	Consumption
Total DOC	1.53±0.13	2.26±0.22	28.91±1.07	28.52±1.03
tDOC	1.53±0.13	0.69±0.08	0.00	0.92±0.05
mDOC	0.00	1.57±0.18	28.91±1.07	27.60±1.01

Table 3. Annual budget (mean ± standard deviations) of relevant biogeochemical processes and proportion of their contribution to the source and sink of DOC in the Changjiang Estuary.

Source and sink	Terms	Bulk (Tg/yr)	Proportion
Production	Bacteria	6.48±0.24	22.42%±0.11%
	Phytoplankton	15.29±0.62	52.91%±0.10%
	Zooplankton	7.13±0.32	24.67%±0.16%
Consumption	Bacteria (Marine)	27.60±1.10	96.79%±0.17%
	Bacteria (Terrigenous)	0.86±0.05	3.01%±0.17%
	Photolysis (Terrigenous)	0.060±0.005	0.20%±0.01%

To figure out the relative contribution of each biogeochemical process in the source and sink of DOC, the annual production and consumption of these processes are calculated. Results shown in Table 3 indicate that the ranks of the processes contributing to the production of DOC are phytoplankton excretion, zooplankton excretion, and bacterial excretion, with respective proportions of 52.91%, 24.67%, and 22.42%, respectively. In the consumption category, the processes ranked from highest to lowest contribution are bacterial uptake of mDOC, bacterial uptake of tDOC, and photolysis, with respective proportions of 96.79%, 3.01%, and 0.20%. Based on the data above, it is evident that bacteria play a predominant role as the primary consumers in the degradation of tDOC, while the contribution of photolysis consumption is relatively minor in the whole estuary.

4 Discussion

4.1 The role of estuaries in mediating DOC flux between land and ocean

Our study employed a physics-biogeochemistry coupled model to investigate the transport and transformation of DOC in the Changjiang Estuary. Although previous studies have included simulations of DOC in estuaries (Anderson et al., 2019; Clark et al., 2022; Druon et al., 2010), they have not explicitly addressed the transport and transformation based on different source-to-sink pathways of terrigenous and marine DOC within a three-dimensional model of the river-estuary-ocean continuum. Our results reveal variations in the rates of distinct processes and their contribution proportions in the Changjiang Estuary, that the Changjiang Estuary plays a vital role in mediating the DOC flux between the land ocean interface, not only as an important transport route for export of terrigenous DOC to open ocean but also as a reactor for biogeochemical cycling of DOC from both terrigenous and marine origins.

Existing literature reveals that a significant part of tDOC delivered from rivers worldwide is depleted before entering the open ocean (Opsahl and Benner, 1997; Looman et al., 2019; Friedlingstein et al., 2023). This signifies that tDOC is removed (mineralized) by biological or abiotic processes within the estuary. A study of the Mississippi-Atchafalaya River system by Fichot and Benner (2014) suggested that biomineralization is the main process for the removal of tDOC in the system, and around ~40% of tDOC is removed during the transport towards the continental shelf within the estuary. Similar results estimated that the removal of tDOC in the Mississippi River estuary is no less than 30-50% within high-salinity (>25 PSU) water mixing (Wang et al., 2004). In the York River estuary, Raymond and Bauer (2000) report the proportion of tDOC removed by bacteria is ~10%. Additional studies have also substantiated that estuaries serve as a reactor and filter for DOC cycling. A study of the Pearl River estuary by He et al. (2010) suggested microbial degradation as the primary bioprocess for the removal of DOC (~31% in the mixing zone). Another study reveals the loss of DOC in the Lena River estuary can reach ~10-20% (Alling et al., 2010). Dai et al. (2012) estimated the removal of DOC in the Artic estuaries to be approximately 20%. Kumar et al. (2022) suggested that during the dry season, the Godavari estuary could remove ~33% DOC by photodegradation and microbial respiration. In the Changjiang Estuary, a series of 12-day incubation experiments showed that ~17% of estuarine DOC were removed after biodegradation (Guo et al., 2021). Surface microbial incubations showed

that the deletion of DOC varied between 5% and 39% (Ji et al., 2021). In our simulations, results indicate that the removal of tDOC can reach ~60% at an annual scale.

Our results (Fig. 9) show that fluctuations of the net cycling rate of DOC, especially between negative and positive values, mainly occur off the estuarine river mouth, namely the plume region and adjacent coastal waters, whilst within the river channel and around the river mouth the net cycling rate remains relatively stable and persistently negative throughout the year. Raymond and Bauer (2001) estimated that, despite around half of tDOC being depleted, the York River Estuary acts as a net source of DOC due to the supplementation of autochthonous mDOC. Our result showing the main contribution of phytoplankton to the export of estuarine DOC is consistent with this study. In addition, a slight loss of DOC at low salinity and a primary source at mid salinity found in the plume of the Changjiang Estuary found in our results also show similarity with the study from the Mississippi River by Fichot and Benner (2014). Our study distinguished between terrigenous and marine components of DOC and applied them to a three-dimensional hydrodynamic-biological model to evaluate the transport and transformation of DOC in the river-estuary-ocean continuum. Our results emphasize that terrestrial DOC undergoes photodegradation and microbial decomposition, with up to 60% of the riverine input being consumed before reaching the ocean, which resulting in the transition of DOC from terrigenous-source dominant to marine-source dominant in the plume area. In contrast, mDOC makes a larger contribution to export, especially from phytoplankton production.

4.2 Factors influencing DOC lability

In our study, it was considered that terrigenous DOM contains more aromatic compounds, leading to the component of T_1 undergoing photochemical reactions at the surface layer. In actual experiments and observations, DOC exposed to sunlight undergoes a certain degree of photo-transformation and becomes more biologically labile. The model considers that a portion of T_1, after photolysis, transitions into the more microbially labile T_2 pool (Text S1). However, this consideration remains somewhat simplified, as some studies have reported the complexity of DOC reactivity during~~following~~ photo-transformation (Medeiros et al., 2015a; Aarnos et al., 2018). ~~tDOC contains a higher proportion of aromatic compounds, which is more prone to photolysis. This consideration of the photolysis process on the surface layer, however, is somewhat simplified. Microbial processing and metabolism in the ocean may produce byproducts such as chromophoric dissolved organic matter (CDOM), which plays a key role in DOM photodegradation (Romera-Castillo et al., 2011; Kinsey et al., 2018). Additionally, CDOM could be a byproduct of of nutrient induced primary productivity (Del Castillo et al., 2000). This indicates that there is a small fraction of DOC in the ocean may turn over by photodegradation. The refractory DOC in the deep sea is resistant to biological degradation. As large scale ocean circulation brings it to the surface, it becomes more susceptible to photolysis (Medeiros et al., 2015a; Mopper et al., 1991). Anderson et al. (2019) developed a one-dimensional model with a simple physical framework to simulate the fate of DOC. This model assumed that 20% of autochtonous DOC would undergo photodegradation, contributing to 13% of the resulting loss. Moreover,~~ Eexperimental evidence indicates that photodegradation can significantly impact subsequent biodegradation by producing biologically labile substrates (Benner and Kaiser, 2011; Mopper and Kieber, 2002). ~~-~~The photo-transformed, biologically labile DOM components may enhance

24

bacterial productivity, as indicated by the increase in unsaturated aliphatic observed in near-surface waters (Medeiros et al., 2015a). Sunlight could significantly impact the biodegradation of DOM in streams, particularly semi-labile DOM, indicating that sunlight not only alters the chemical structure of DOM but also changes its susceptibility to microbial degradation (Bowen et al., 2020). These findings indicate that photodegradation and biodegradation processes can mutually influence each other.

In addition to photodegradation increasing the biological lability of DOC, the priming effect also influences DOC transport from rivers to the ocean. This effect occurs when labile organic matter interacts with stable organic matter, altering the mineralization rate of the latter (Bianchi, 2011; Sanches et al., 2021). The priming effect may likewise be induced by bacteria and archaea, utilizing various pools of organic carbon (Kirchman et al., 2007). The addition of algal DOC or trehalose in laboratory microcosm experiments has demonstrated that the priming effect significantly enhances the remineralization rate of tDOC (Bianchi et al., 2015). A substantial positive priming effect (15%–34% of initial stable DOM) occurred exclusively with the presence of mixed labile DOM (glucose and amino acids) or complex labile DOM (disaccharide) in incubation experiments, which is temporary and lasting for around two weeks (Laffet et al., 2023). Labile organic matter enhances microbial metabolism and enzyme production, thereby altering the mineralization of refractory DOC (Guenet et al., 2010). Besides the influence of labile DOC addition on the lability of refractory DOC, the impact of other environmental factors has also drawn attention. For example, the existence of sediments in the incubation did not increase the priming effect (Laffet et al., 2023). In a 346-day incubation experiment where the native microbial assemblage of the Atlantic was replaced with a coastal microbial assemblage, it was found that coastal microbes consumed 2.3-8.7% of the refractory DOC (Shen and Benner, 2018), indicating different microbial communities have varying effects on refractory DOC (Carlson et al., 2004). Additionally, other research indicates that microbes can degrade more refractory compounds, which exhibit higher temperature sensitivity (Lønborg et al., 2018). These studies indicate that the reactivity of DOC is influenced by various factors, leaving substantial scope for further theoretical and experimental and modeling research.

4.3 Distribution pattern of DOC between summer and winter

The hydrodynamic and ecological environments of the Changjiang Estuary exhibit representative characteristics in both summer and winter. Moreover, most observational voyages are concentrated in these two seasons. Therefore, our study focuses on the distributions and source-sink patterns of DOC during summer and winter. The average concentration of DOC in summer and winter across the salinity gradient (Fig. 10.) indicates that DOC concentration gradually decreases from freshwater to saltwater. DOC in winter exhibits more conservative mixing at low- and mid-salinity compared to summer. Near the plume region, the influence of the DOC source becomes significant. The change in the slope of the curve is more pronounced in the summer, indicating that the source-sink variations are more pronounced in summer compared to winter. This seasonal variation is closely linked to the hydrological environment and biological activities in the estuary. In the summer, the mixing in the Changjiang Estuary is relatively weaker compared to winter, resulting in a deeper euphotic zone that benefits the primary production activities of phytoplankton (Zhu et al., 2009). Chlorophyll-a concentrations are higher in

25

summer than in winter, which depends on temperature and nutrient levels, with higher river discharge in summer (Yang et al., 2014; Liu et al., 2016). In the ECS, it was observed that the growth rates of phytoplankton correlate positively with surface water temperature. Microzooplankton grazing effectively regulated primary production in summer, whereas grazing activity was minimal in winter due to the colder temperature (Zheng et al., 2015). Simultaneously, the seasonal pattern of planktonic bacterial productivity is similar to that of water temperature, resulting in higher rates during the summer (Peierls and Paerl, 2010). (Wang et al., 2010; Chai et al., 2006)Research indicates that higher inflow with more DOC loading would stimulate heterotrophic bacterioplankton production in the upper estuary (Hitchcock et al., 2010; Letourneau and Medeiros, 2019). Bacterial respiration and production are intimately connected to DOC originating from plankton. In summer, peak rates are frequently observed at mid-salinity levels in waters with elevated carbohydrate concentrations (Benner and Opsahl, 2001; Kinsey et al., 2018). The observed increase in DOC around the edge of plume area, which is more pronounced in summer than in winter, is consistent with previous research findings (Song et al., 2017; Shen et al., 2016; Guo et al., 2021). Our results further explain the transport variations of tDOC from river inputs and mDOC within the estuary, as well as quantify the contributions of phytoplankton, zooplankton, and bacteria to estuarine DOC.(Wang et al., 2010)
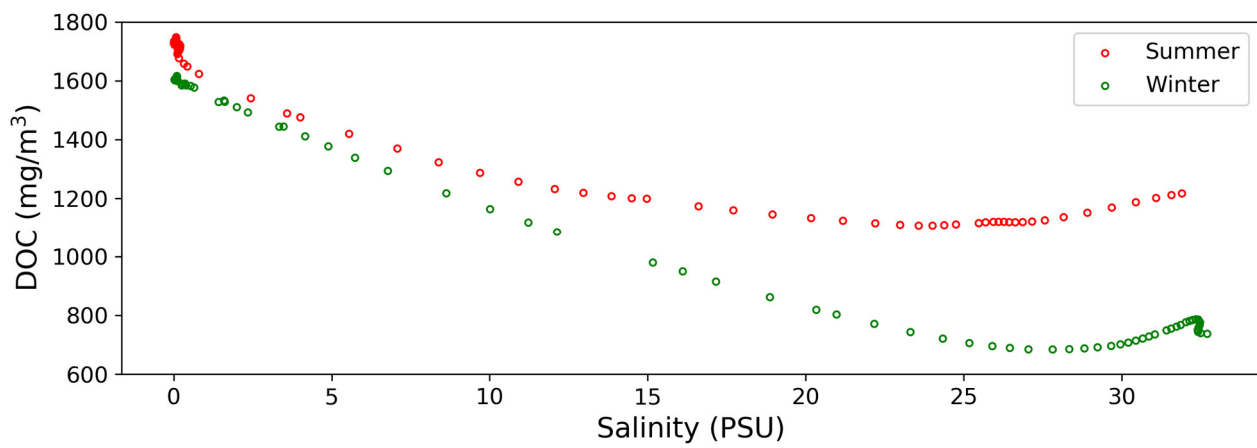
Figure 10. The surface average DOC varies along the profile (Fig. 2) as it mixes with the salinity gradient in summer and winter in the model.

4.2 4 Future research needsLimitations and future research needs

The considerations of our model regarding sediment flocculation and adsorption are relatively simple by assuming a constant rate (Table S1) and may require further development and improvement. The quantitative impact of flocculation on DOC in the Changjiang Estuary remains unknown. We assume that the simplifications have a limited effect on the cycling of DOC in the estuary, as indicated by studies from other estuaries. For example, Søndergaard et al. (2003) found that the flocculation of DOC with a salinity gradient ranging from 0 to 25 ppt was not a primary removal process, resulting in only a marginal decrease of 2-5%. In another study by (Khoo et al., 2022), the flocculation removal of DOC within a salinity range of 12-25 PSU was also found to constitute a minor proportion (~3.5%). In this study, the atmospheric pCO2 of 385 ppm was slightly

underestimated (Li et al., 2018; Guo et al., 2015). We adjusted the model configuration to set pCO2 at 400ppm with an increase 3 ppm per year for sensitivity experiment. The model results indicate that the DOC concentration level remained almost unchanged. This may be attributed to the deviation is too small to reach the threshold that would cause changes in DOC (James et al., 2017). Cultivation experiments on marine picocyanobacterial were conducted under ambient (380 ppmv) and elevated (1000 ppmv) CO_2 levels. The results indicated a reduction in cellular chlorophyll a, but no changes in DOC were observed (Mou et al., 2017). Additionally, the DOC in model exhibits limitations in effectively capturing the north-eastward expansion of DOC during the summer (Fig. S1). This inconsistency may be attributed to the uncertainties in both measurement and modeling, including the uncertainty in sampling time, as most of the sampling data only covered a few days within a month. Additionally, there were variations in the locations where data was collected, with some points having more data collected than others, and there was limited availability of collected data. Nevertheless, a general agreement in the DOC concentration between model and observational data is shown.

Research on the cycling of DOC in the river-estuary-ocean continuum is essential for understanding carbon dynamics and coastal ecosystems, particularly in the context of intensified human activities on land and ocean, as well as global warming-induced change in the occurrence of extreme climate events. With increased extreme climatic events, estuaries are susceptible to changes in nutrient and organic matter transport and transformations, which impact the structure and function of estuarine ecosystems (Wetz and Yoskowitz, 2013; Leal Filho et al., 2022). As a key component of ecosystems, the transformation, variation, and potential ecological effects of DOC in estuaries require further investigation. Ongoing human activities are causing continuous changes in many estuarine and coastal ecosystems (Cloern et al., 2016). The long-term trends and potential shifts in DOC cycling in estuaries under human influence also need further investigation.

5 Conclusions

A physical-biogeochemical coupled model FVCOM-ERSEM was employed to simulate the sources and sink of DOC in the Changjiang Estuary. Through an analysis of variation, transformation, and budget estimation of DOC in the river-estuary-ocean continuum, we derived insights into the influencing factors of DOC from both terrigenous and marine origins in the Changjiang Estuary. Additionally, we identified patterns of source-sink variations in the DOC dynamics. The primary conclusions drawn from our study are as follows:

During summer, the distribution of DOC is jointly governed by hydrodynamic and biogeochemical processes, whereas in winter, it is mainly controlled by hydrodynamics. Within the Changjiang Estuary, the river channel and river mouth are primarily dominated by tDOC, while the plume and open shelf region are dominated by mDOC.

In summer, the plume region serves as a transitional zone where the dominated source of DOC shifts from terrigenous to marine origin, as well as a shift from a sink to a source along the river-estuary-ocean continuum. The transition from terrigenous-dominated to marine-dominated DOC occurs primarily around a salinity contour line of 20 PSU. Furthermore,

the offshore coastal region predominantly acts as a source, characterized by a higher DOC production rate. In winter, a vast part (>90%) of the estuary functions as a sink.

475 Analysis of the budget of terrigenous and marine components suggests that the majority of tDOC (~55%) undergoes depletion within the Changjiang Estuary at an annual scale. DOC exported to the open ocean mainly originates from mDOC. The proportions of tDOC and mDOC export are approximately 31% and 69%, respectively. Based on our results, it can be inferred that the biogeochemical processes within the Changjiang Estuary play a crucial role in supporting the production and export of DOC to the open ocean. Overall, phytoplankton emerges as the primary contributor to the generation and

480 export of estuarine DOC, and the gradient variations of chlorophyll-a serve as practical indicators of the source-sink transitions.

Open Research.   The FVCOM-ERSEM code and documentation is open access and can be found on the links below:

490 FVCOM: https://github.com/FVCOM-GitHub/FVCOM/releases;

ERSEM: https://github.com/pmlmodelling/ersem/.

Previous related results in FVCOM-ERSEM in the Changjiang Estuary published online:

https://figshare.com/s/ab600431c5958ee9d261 (Interannual variabilities of nutrients and phytoplankton off the Changjiang Estuary in response to Changing River inputs);

495 https://figshare.com/s/243b4e8417b7bd0106d8 (Influence of suspended sediment front on nutrients and phytoplankton dynamics off the Changjiang Estuary: A FVCOM-ERSEM coupled model experiment).

Data availability. Data are available from the corresponding author upon reasonable request.

500 *Author contribution.* JG, WZ and JY designed the study and performed the research. JY conducted the analysis and wrote the first draft of the manuscript, CZ and JY conducted the methodology. JG and WZ supervised this study. All the authors contributed to revisions and discussion.

Competing interests. The contact author has declared that neither of the authors has any competing interests.

References

Aarnos, H., Gélinas, Y., Kasurinen, V., Gu, Y., Puupponen, V.-M., and Vähätalo, A. V.: Photochemical Mineralization of Terrigenous DOC to Dissolved Inorganic Carbon in Ocean, Global Biogeochemical Cycles, 32, 250-266, doi: 10.1002/2017gb005698, 2018.

Alling, V., Sanchez-Garcia, L., Porcelli, D., Pugach, S., Vonk, J. E., van Dongen, B., Mörth, C. M., Anderson, L. G., Sokolov, A., Andersson, P., Humborg, C., Semiletov, I., and Gustafsson, Ö.: Nonconservative behavior of dissolved organic carbon across the Laptev and East Siberian seas, Global Biogeochemical Cycles, 24, doi: 10.1029/2010gb003834, 2010.

Anderson, T. R., Rowe, E. C., Polimene, L., Tipping, E., Evans, C. D., Barry, C. D. G., Hansell, D. A., Kaiser, K., Kitidis, V., Lapworth, D. J., Mayor, D. J., Monteith, D. T., Pickard, A. E., Sanders, R. J., Spears, B. M., Torres, R., Tye, A. M., Wade, A. J., and Waska, H.: Unified concepts for understanding and modelling turnover of dissolved organic matter from freshwaters to the ocean: the UniDOM model, Biogeochemistry, 146, 105-123, doi: 10.1007/s10533-019-00621-1, 2019.

Asmala, E., Bowers, D. G., Autio, R., Kaartokallio, H., and Thomas, D. N.: Qualitative changes of riverine dissolved organic matter at low salinities due to flocculation, Journal of Geophysical Research: Biogeosciences, 119, 1919-1933, doi: 10.1002/2014jg002722, 2014.

Bauer, J. E. and Bianchi, T. S.: 5.02 - Dissolved Organic Carbon Cycling and Transformation, in: Treatise on Estuarine and Coastal Science, edited by: Wolanski, E., and McLusky, D., Academic Press, Waltham, 7-67, 10.1016/B978-0-12-374711-2.00502-7, 2011.

Bauer, J. E., Cai, W. J., Raymond, P. A., Bianchi, T. S., Hopkinson, C. S., and Regnier, P. A.: The changing carbon cycle of the coastal ocean, Nature, 504, 61-70, doi: 10.1038/nature12857, 2013.

Benner, R. and Kaiser, K.: Biological and photochemical transformations of amino acids and lignin phenols in riverine dissolved organic matter, Biogeochemistry, 102, 209-222, doi: 10.1007/s10533-010-9435-4, 2011.

Benner, R. and Opsahl, S.: Molecular indicators of the sources and transformations of dissolved organic matter in the Mississippi river plume, Organic Geochemistry, 32, 597-611, doi: 10.1016/S0146-6380(00)00197-2, 2001.

Bianchi, T. S.: The role of terrestrially derived organic carbon in the coastal ocean: A changing paradigm and the priming effect, Proceedings of the National Academy of Sciences of the United States of America, 108, 19473-19481, doi: 10.1073/pnas.1017982108, 2011.

Bianchi, T. S., Thornton, D. C. O., Yvon-Lewis, S. A., King, G. M., Eglinton, T. I., Shields, M. R., Ward, N. D., and Curtis, J.: Positive priming of terrestrially derived dissolved organic matter in a freshwater microcosm system, Geophysical Research Letters, 42, 5460-5467, doi: 10.1002/2015GL064765, 2015.

Bowen, J. C., Kaplan, L. A., and Cory, R. M.: Photodegradation disproportionately impacts biodegradation of semi-labile DOM in streams, Limnology and Oceanography, 65, 13-26, doi: 10.1002/lno.11244, 2020.

Bruggeman, J. and Bolding, K.: A general framework for aquatic biogeochemical models, Environmental Modelling & Software, 61, 249-265, doi: 10.1016/j.envsoft.2014.04.002, 2014.

Butenschön, M., Clark, J., Aldridge, J. N., Allen, J. I., Artioli, Y., Blackford, J., Bruggeman, J., Cazenave, P., Ciavatta, S., Kay, S., Lessin, G., van Leeuwen, S., van der Molen, J., de Mora, L., Polimene, L., Sailley, S., Stephens, N., and Torres, R.:

540   ERSEM 15.06: a generic model for marine biogeochemistry and the ecosystem dynamics of the lower trophic levels, Geoscientific Model Development, 9, 1293-1339, doi: 10.5194/gmd-9-1293-2016, 2016.

Carlson, C. A. and Hansell, D. A.: DOM Sources, Sinks, Reactivity, and Budgets, Biogeochemistry of Marine Dissolved Organic Matter, 2nd Edition, 65-126 pp., 10.1016/b978-0-12-405940-5.00003-0, 2015.

Carlson, C. A., Giovannoni, S. J., Hansell, D. A., Goldberg, S. J., Parsons, R., and Vergin, K.: Interactions among dissolved

545   organic carbon, microbial processes, and community structure in the mesopelagic zone of the northwestern Sargasso Sea, Limnology and Oceanography, 49, 1073-1083, doi: 10.4319/lo.2004.49.4.1073, 2004.

Catalán, N., Marcé, R., Kothawala, D. N., and Tranvik, L. J.: Organic carbon decomposition rates controlled by water retention time across inland waters, Nature Geoscience, 9, 501-504, doi: 10.1038/NGEO2720, 2016.

Chai, C., Yu, Z., Song, X., and Cao, X.: The Status and Characteristics of Eutrophication in the Yangtze River (Changjiang)

550   Estuary and the Adjacent East China Sea, China, Hydrobiologia, 563, 313-328, doi: 10.1007/s10750-006-0021-7, 2006.

Chen, C., Liu, H., and Beardsley, R. C.: An unstructured grid, finite-volume, three-dimensional, primitive equations ocean model: application to coastal ocean and estuaries, Journal of Atmospheric Oceanic Technology, 20, 159-186, doi: 10.1175/1520-0426(2003)020<0159:AUGFVT>2.0.CO;2, 2003.

Chen, C., Beardsley, R., Cowles, G., Qi, J., Lai, Z., Gao, G., Stuebe, D., Xu, Q., Xue, P., and Ge, J.: An unstructured grid,

555   finite-volume community ocean model FVCOM User Manual, SMAST/UMASSD Technical Report 13-0701, 2013.

Clark, J. B., Mannino, A., Tzortziou, M., Spencer, R. G. M., and Hernes, P.: The Transformation and Export of Organic Carbon Across an Arctic River-Delta-Ocean Continuum, Journal of Geophysical Research: Biogeosciences, 127, e2022JG007139, doi: 10.1029/2022JG007139, 2022.

Cloern, J. E., Abreu, P. C., Carstensen, J., Chauvaud, L., Elmgren, R., Grall, J., Greening, H., Johansson, J. O. R., Kahru, M.,

560   Sherwood, E. T., Xu, J., and Yin, K.: Human activities and climate variability drive fast-paced change across the world's estuarine-coastal ecosystems, Global Change Biology, 22, 513-529, doi: 10.1111/gcb.13059, 2016.

Dai, M., Yin, Z., Meng, F., Liu, Q., and Cai, W.: Spatial distribution of riverine DOC inputs to the ocean: an updated global synthesis, Current Opinion in Environmental Sustainability, 4, 170-178, doi: 10.1016/j.cosust.2012.03.003, 2012.

Del Castillo, C. E., Gilbes, F., Coble, P. G., and Müller-Karger, F. E.: On the dispersal of riverine colored dissolved organic

565   matter over the West Florida Shelf, 45, 1425-1432, doi: https://doi.org/10.4319/lo.2000.45.6.1425, 2000.

Druon, J. N., Mannino, A., Signorini, S., McClain, C., Friedrichs, M., Wilkin, J., and Fennel, K.: Modeling the dynamics and export of dissolved organic matter in the Northeastern U.S. continental shelf, Estuarine, Coastal and Shelf Science, 88, 488-507, doi: 10.1016/j.ecss.2010.05.010, 2010.

Evans, C. D., Futter, M. N., Moldan, F., Valinia, S., Frogbrook, Z., and Kothawala, D. N.: Variability in organic carbon

570   reactivity across lake residence time and trophic gradients, Nature Geoscience, 10, 832-835, doi: 10.1038/NGEO3051, 2017.

Fellman, J. B., Spencer, R. G. M., Hernes, P. J., Edwards, R. T., D'Amore, D. V., and Hood, E.: The impact of glacier runoff

on the biodegradability and biochemical composition of terrigenous dissolved organic matter in near-shore marine ecosystems, Marine Chemistry, 121, 112-122, doi: 10.1016/j.marchem.2010.03.009, 2010.

Fichot, C. G. and Benner, R.: The fate of terrigenous dissolved organic carbon in a river-influenced ocean margin, Global Biogeochemical Cycles, 28, 300-318, doi: 10.1002/2013gb004670, 2014.

Friedlingstein, P., O'Sullivan, M., Jones, M. W., Andrew, R. M., Bakker, D. C. E., Hauck, J., Landschützer, P., Le Quéré, C., Luijkx, I. T., Peters, G. P., Peters, W., Pongratz, J., Schwingshackl, C., Sitch, S., Canadell, J. G., Ciais, P., Jackson, R. B., Alin, S. R., Anthoni, P., Barbero, L., Bates, N. R., Becker, M., Bellouin, N., Decharme, B., Bopp, L., Brasika, I. B. M., Cadule, P., Chamberlain, M. A., Chandra, N., Chau, T. T. T., Chevallier, F., Chini, L. P., Cronin, M., Dou, X. Y., Enyo, K., Evans, W., Falk, S., Feely, R. A., Feng, L., Ford, D. J., Gasser, T., Ghattas, J., Gkritzalis, T., Grassi, G., Gregor, L., Gruber, N., Gürses, Ö., Harris, I., Hefner, M., Heinke, J., Houghton, R. A., Hurtt, G. C., Iida, Y., Ilyina, T., Jacobson, A. R., Jain, A., Jarníková, T., Jersild, A., Jiang, F., Jin, Z., Joos, F., Kato, E., Keeling, R. F., Kennedy, D., Goldewijk, K. K., Knauer, J., Korsbakken, J. I., Körtzinger, A., Lan, X., Lefèvre, N., Li, H. M., Liu, J. J., Liu, Z. Q., Ma, L., Marland, G., Mayot, N., McGuire, P. C., McKinley, G. A., Meyer, G., Morgan, E. J., Munro, D. R., Nakaoka, S. I., Niwa, Y., O'Brien, K. M., Olsen, A., Omar, A. M., Ono, T., Paulsen, M., Pierrot, D., Pocock, K., Poulter, B., Powis, C. M., Rehder, G., Resplandy, L., Robertson, E., Rödenbeck, C., Rosan, T. M., Schwinger, J., Séférian, R., Smallman, T. L., Smith, S. M., Sospedra-Alfonso, R., Sun, Q., Sutton, A. J., Sweeney, C., Takao, S., Tans, P. P., Tian, H. Q., Tilbrook, B., Tsujino, H., Tubiello, F., van der Werf, G. R., van Ooijen, E., Wanninkhof, R., Watanabe, M., Wimart-Rousseau, C., Yang, D. X., Yang, X. J., Yuan, W. P., Yue, X., Zaehle, S., Zeng, J. Y., and Zheng, B.: Global Carbon Budget 2023, Earth System Science Data, 15, 5301-5369, doi: 10.5194/essd-15-5301-2023, 2023.

Gao, L., Gao, Y., Song, S., and Zhang, F.: Non-conservative behavior of dissolved organic carbon in the Changjiang (Yangtze River) Estuary and the adjacent East China Sea, Continental Shelf Research, 197, doi: 10.1016/j.csr.2020.104084, 2020.

Ge, J., Shen, F., Guo, W., Chen, C., and Ding, P.: Estimation of critical shear stress for erosion in the C hangjiang E stuary: A synergy research of observation, GOCI sensing and modeling, Journal of Geophysical Research: Oceans, 120, 8439-8465, doi: 10.1002/2015JC010992, 2015.

Ge, J., Ding, P., Chen, C., Hu, S., Fu, G., and Wu, L.: An integrated East China Sea-Changjiang Estuary model system with aim at resolving multi-scale regional-shelf-estuarine dynamics, Ocean Dynamics, 63, 881-900, doi: 10.1007/s10236-013-0631-3, 2013.

Ge, J., Zhou, Z., Yang, W., Ding, P., Chen, C., Wang, Z. B., and Gu, J.: Formation of Concentrated Benthic Suspension in a Time-Dependent Salt Wedge Estuary, Journal of Geophysical Research: Oceans, 123, 8581-8607, doi: 10.1029/2018jc013876, 2018.

Ge, J., Torres, R., Chen, C., Liu, J., Xu, Y., Bellerby, R., Shen, F., Bruggeman, J., and Ding, P.: Influence of suspended sediment front on nutrients and phytoplankton dynamics off the Changjiang Estuary: A FVCOM-ERSEM coupled model experiment, Journal of Marine Systems, 204, 103292, doi: 10.1016/j.jmarsys.2019.103292, 2020.

31

Gu, H., Moore, W., Zhang, L., Du, J., and Zhang, J.: Using radium isotopes to estimate the residence time and the contribution of submarine groundwater discharge (SGD) in the Changjiang effluent plume, East China Sea, Continental Shelf Research, 35, 95-107, doi: 10.1016/j.csr.2012.01.002, 2012.

Guenet, B., Danger, M., Abbadie, L., and Lacroix, G.: Priming effect: bridging the gap between terrestrial and aquatic ecology, Ecology, 91, 2850-2861, doi: 10.1890/09-1968.1, 2010.

Guo, J., Liang, S., Wang, X., and Pan, X.: Distribution and dynamics of dissolved organic matter in the Changjiang Estuary and adjacent sea, Journal of Geophysical Research: Biogeosciences, 126, doi: 10.1029/2020jg006161, 2021.

Guo, J., Liang, S., Li, X., Li, W., Wang, Y., and Su, R.: Composition and bioavailability of dissolved organic matter in different water masses of the East China sea, Estuarine, Coastal and Shelf Science, 212, 189-202, doi: 10.1016/j.ecss.2018.07.009, 2018.

Guo, W., Yang, L., Zhai, W., Chen, W., Osburn, C. L., Huang, X., and Li, Y.: Runoff-mediated seasonal oscillation in the dynamics of dissolved organic matter in different branches of a large bifurcated estuary-The Changjiang Estuary, Journal of Geophysical Research: Biogeosciences, 119, 776-793, doi: 10.1002/2013jg002540, 2014.

Guo, X. H., Zhai, W. D., Dai, M. H., Zhang, C., Bai, Y., Xu, Y., Li, Q., and Wang, G. Z.: Air–sea CO_2 fluxes in the East China Sea based on multiple-year underway observations, Biogeosciences, 12, 5495-5514, doi: 10.5194/bg-12-5495-2015, 2015.

Han, L., Wang, Y., Xu, Y., Wang, Y., Zheng, Y., and Wu, J.: Water- and base-extractable organic matter in sediments from lower Yangtze River–Estuary–East China Sea continuum: insight into accumulation of organic carbon in the river-dominated margin, Frontiers in Marine Science, 35, 95-107, doi: 10.3389/fmars.2021.617241, 2021.

Hansell, D. A.: Recalcitrant Dissolved Organic Carbon Fractions, in: Annual Review of Marine Science, Vol 5, edited by: Carlson, C. A., and Giovannoni, S. J., Annual Review of Marine Science, 421-445, 10.1146/annurev-marine-120710-100757, 2013.

Hansell, D. A., Carlson, C. A., Repeta, D. J., and Schlitzer, R.: Dissolved organic matter in the ocean: A controversy stimulates new insights, Oceanography, 22, 202-211, doi: www.jstor.org/stable/24861036, 2009.

He, W., Chen, M., Schlautman, M. A., and Hur, J.: Dynamic exchanges between DOM and POM pools in coastal and inland aquatic ecosystems: A review, Science of The Total Environment, 551-552, 415-428, doi: 10.1016/j.scitotenv.2016.02.031, 2016.

Helms, J. R., Stubbins, A., Ritchie, J. D., Minor, E. C., Kieber, D. J., and Mopper, K.: Absorption spectral slopes and slope ratios as indicators of molecular weight, source, and photobleaching of chromophoric dissolved organic matter, Limnology and Oceanography, 53, 955-969, doi: 10.4319/lo.2008.53.3.0955, 2008.

Herrmann, M., Najjar, R. G., Kemp, W. M., Alexander, R. B., Boyer, E. W., Cai, W. J., Griffith, P. C., Kroeger, K. D., McCallister, S. L., and Smith, R. A.: Net ecosystem production and organic carbon balance of U.S. East Coast estuaries: A synthesis approach, Global Biogeochemical Cycles, 29, 96-111, doi: 10.1002/2013gb004736, 2015.

Hitchcock, J. N., Mitrovic, S. M., Kobayashi, T., and Westhorpe, D. P.: Responses of Estuarine Bacterioplankton,

640   Phytoplankton and Zooplankton to Dissolved Organic Carbon (DOC) and Inorganic Nutrient Additions, Estuaries and Coasts, 33, 78-91, doi: 10.1007/s12237-009-9229-x, 2010.

Hopkinson, C. S. and Vallino, J. J.: Efficient export of carbon to the deep ocean through dissolved organic matter, Nature, 433, 142-145, doi: 10.1038/nature03191, 2005.

Hu, J., Zou, L., Wang, J., Ren, Q., Xia, B., and Yu, G.: Factors regulating the compositions and distributions of dissolved
645   organic matter in the estuaries of Jiaozhou Bay in North China, Oceanologia, 62, 101-110, doi: 10.1016/j.oceano.2019.09.002, 2020.

Hudson, N., Baker, A., and Reynolds, D.: Fluorescence analysis of dissolved organic matter in natural, waste and polluted waters—a review, River Research and Applications, 23, 631-649, doi: 10.1002/rra.1005, 2007.

James, A. K., Passow, U., Brzezinski, M. A., Parsons, R. J., Trapani, J. N., and Carlson, C. A.: Elevated pCO2 enhances
650   bacterioplankton removal of organic carbon, Plos One, 12, e0173145, doi: 10.1371/journal.pone.0173145, 2017.

Ji, C., Chen, Y., and Yang, G.: Seasonal variation, degradation, and bioavailability of dissolved organic matter in the Changjiang Estuary and its adjacent East China Sea, Journal of Geophysical Research: Oceans, 126, doi: 10.1029/2020jc016648, 2021.

Jiao, N. and Azam, F.: Microbial carbon pump and its significance for carbon sequestration in the ocean, Microbial Carbon
655   Pump in the Ocean, 10, 43-45, 2011.

Jiao, N., Herndl, G. J., Hansell, D. A., Benner, R., Kattner, G., Wilhelm, S. W., Kirchman, D. L., Weinbauer, M. G., Luo, T., Chen, F., and Azam, F.: Microbial production of recalcitrant dissolved organic matter: long-term carbon storage in the global ocean, Nature Reviews Microbiology, 8, 593-599, doi: 10.1038/nrmicro2386, 2010.

Jiao, N., Robinson, C., Azam, F., Thomas, H., Baltar, F., Dang, H., Hardman-Mountford, N. J., Johnson, M., Kirchman, D. L.,
660   Koch, B. P., Legendre, L., Li, C., Liu, J., Luo, T., Luo, Y. W., Mitra, A., Romanou, A., Tang, K., Wang, X., Zhang, C., and Zhang, R.: Mechanisms of microbial carbon sequestration in the ocean – future research directions, Biogeosciences, 11, 5285-5306, doi: 10.5194/bg-11-5285-2014, 2014.

Khoo, C. L. L., Sipler, R. E., Fudge, A. R., Beheshti Foroutani, M., Boyd, S. G., and Ziegler, S. E.: Salt-induced flocculation of dissolved organic matter and Iron is controlled by their concentration and ratio in boreal coastal systems, Journal of
665   Geophysical Research: Biogeosciences, 127, doi: 10.1029/2022jg006844, 2022.

Kinsey, J. D., Corradino, G., Ziervogel, K., Schnetzer, A., and Osburn, C. L. J. F. i. M. S.: Formation of chromophoric dissolved organic matter by bacterial degradation of phytoplankton-derived aggregates, Frontiers in Marine Science, 4, 430, doi: 10.3389/fmars.2017.00430, 2018.

Kirchman, D. L., Elifantz, H., Dittel, A. I., Malmstrom, R. R., and Cottrell, M. T.: Standing stocks and activity of Archaea
670   and Bacteria in the western Arctic Ocean, Limnology and Oceanography, 52, 495-507, doi: 10.4319/lo.2007.52.2.0495, 2007.

Kumar, B. S. K., Sarma, V. V. S. S., and Cardinal, D.: Tracing terrestrial versus marine sources of dissolved organic carbon in the largest monsoonal Godavari estuary in India using stable carbon isotopes, Estuarine, Coastal and Shelf Science, 276, doi: 10.1016/j.ecss.2022.108004, 2022.

33

Laffet, W., Prentice, A., and Tremblay, L.: Evidence for a Temporary Positive Priming Effect in Aquatic Systems With

675   Certain Substrates and Isotopic Discrimination of DOM Sources, Journal of Geophysical Research: Biogeosciences, 128, doi: 10.1029/2023jg007534, 2023.

Le, C. F. and Hu, C. M.: A hybrid approach to estimate chromophoric dissolved organic matter in turbid estuaries from satellite measurements: A case study for Tampa Bay, Optics Express, 21, 18849-18871, doi: 10.1364/oe.21.018849, 2013.

Leal Filho, W., Nagy, G. J., Martinho, F., Saroar, M., Erache, M. G., Primo, A. L., Pardal, M. A., and Li, C.: Influences of

680   climate change and variability on estuarine ecosystems: an impact study in selected European, South American and Asian countries, International Journal of Environmental Research and Public Health, 19, 585, doi: 10.3390/ijerph19010585, 2022.

Letourneau, M. L. and Medeiros, P. M.: Dissolved Organic Matter Composition in a Marsh-Dominated Estuary: Response to Seasonal Forcing and to the Passage of a Hurricane, Journal of Geophysical Research: Biogeosciences, 124, 1545-1559, doi: 10.1029/2018JG004982, 2019.

685   Li, D., Chen, J., Ni, X., Wang, K., Zeng, D., Wang, B., Jin, H., Huang, D., and Cai, W.-J.: Effects of Biological Production and Vertical Mixing on Sea Surface pCO_2 Variations in the Changjiang River Plume During Early Autumn: A Buoy-Based Time Series Study, Journal of Geophysical Research: Oceans, 123, 6156-6173, doi: 10.1029/2017JC013740, 2018.

Li, P., Chen, L., Zhang, W., and Huang, Q.: Spatiotemporal distribution, sources, and photobleaching imprint of dissolved organic matter in the Yangtze Estuary and its adjacent sea using fluorescence and parallel factor analysis, Plos One, 10, doi:

690   10.1371/journal.pone.0130852, 2015.

Liu, D., Bai, Y., He, X., Pan, D., Chen, C.-T. A., Li, T., Xu, Y., Gong, C., and Zhang, L.: Satellite-derived particulate organic carbon flux in the Changjiang River through different stages of the Three Gorges Dam, Remote Sensing of Environment, 223, 154-165, doi: 10.1016/j.rse.2019.01.012, 2019.

Liu, Q., Pan, D., Bai, Y., Wu, K., Chen, C.-T. A., Liu, Z., and Zhang, L.: Estimating dissolved organic carbon inventories in

695   the East China Sea using remote-sensing data, Journal of Geophysical Research: Oceans, 119, 6557-6574, doi: 10.1002/2014jc009868, 2014.

Liu, X., Xiao, W., Landry, M. R., Chiang, K.-P., Wang, L., and Huang, B.: Responses of Phytoplankton Communities to Environmental Variability in the East China Sea, Ecosystems, 19, 832-849, doi: 10.1007/s10021-016-9970-5, 2016.

Liu, X., Yang, S., Huang, W., Li, L., Zeng, C., Hu, X., and Teng, F.: Seasonal Transport Characteristics of Suspended

700   Particulate Organic Carbon in the Middle and Lower Yangtze River and the Relationship with Three Georges Reservoir, Advanced Materials Research, 663, 1058-1063, doi: 10.4028/www.scientific.net/AMR.663.1058, 2013.

Lønborg, C., Álvarez–Salgado, X. A., Letscher, R. T., and Hansell, D. A.: Large Stimulation of Recalcitrant Dissolved Organic Carbon Degradation by Increasing Ocean Temperatures, Frontiers in Marine Science, 4, doi: 10.3389/fmars.2017.00436, 2018.

705   Looman, A., Santos, I. R., Tait, D. R., Webb, J., Holloway, C., and Maher, D. T.: Dissolved carbon, greenhouse gases, and δ 13 C dynamics in four estuaries across a land use gradient, Aquatic Sciences, 81, doi: 10.1007/s00027-018-0617-9, 2019.

Ma, M., Zhang, W., Chen, W., Deng, J., and Schrum, C.: Impacts of morphological change and sea-level rise on stratification

in the Pearl River Estuary, Frontiers in Marine Science, 10, doi: 10.3389/fmars.2023.1072080, 2023.

Marcinek, S., Santinelli, C., Cindrić, A.-M., Evangelista, V., Gonnelli, M., Layglon, N., Mounier, S., Lenoble, V., and Omanović, D.: Dissolved organic matter dynamics in the pristine Krka River estuary (Croatia), Marine Chemistry, 225, doi: 10.1016/j.marchem.2020.103848, 2020.

Martineac, R. P., Vorobev, A. V., Moran, M. A., and Medeiros, P. M.: Assessing the Contribution of Seasonality, Tides, and Microbial Processing to Dissolved Organic Matter Composition Variability in a Southeastern U.S. Estuary, Frontiers in Marine Science, 8, doi: 10.3389/fmars.2021.781580, 2021.

Medeiros, P. M., Seidel, M., Powers, L. C., Dittmar, T., Hansell, D. A., and Miller, W. L.: Dissolved organic matter composition and photochemical transformations in the northern North Pacific Ocean, Geophysical Research Letters, 42, 863-870, doi: 10.1002/2014gl062663, 2015a.

Medeiros, P. M., Seidel, M., Ward, N. D., Carpenter, E. J., Gomes, H. R., Niggemann, J., Krusche, A. V., Richey, J. E., Yager, P. L., and Dittmar, T.: Fate of the Amazon River dissolved organic matter in the tropical Atlantic Ocean, Global Biogeochemical Cycles, 29, 677-690, doi: 10.1002/2015gb005115, 2015b.

Meng, Q., Zhang, W., Zhou, F., Liao, Y., Yu, P., Tang, Y., Ma, X., Tian, D., Ding, R., Ni, X., Zeng, D., and Schrum, C.: Water oxygen consumption rather than sediment oxygen consumption drives the variation of hypoxia on the East China Sea shelf, Journal of Geophysical Research: Biogeosciences, 127, doi: 10.1029/2021JG006705, 2022.

Mopper, K. and Kieber, D.: Photochemistry and the Cycling of Carbon, Sulfur, Nitrogen and Phosphorus, in: Biogeochemistry of Marine Dissolved Organic Matter, edited by: Dennis A. Hansell, C. A. C., 455-507, 10.1016/B978-012323841-2/50011-7, 2002.

Mopper, K., Zhou, X., Kieber, R., Kieber, D., Sikorski, R., and Jones, R.: Photochemical degradation of dissolved organic carbon and its impact on the oceanic carbon cycle, Nature, 353, 60-62, doi: 10.1038/353060a0, 1991.

Mou, S., Zhang, Y., Li, G., Li, H., Liang, Y., Tang, L., Tao, J., Xu, J., Li, J., Zhang, C., and Jiao, N.: Effects of elevated CO2 and nitrogen supply on the growth and photosynthetic physiology of a marine cyanobacterium, Synechococcus sp. PCC7002, Journal of Applied Phycology, 29, 1755-1763, doi: 10.1007/s10811-017-1089-3, 2017.

Opsahl, S. and Benner, R.: Distribution and cycling of terrigenous dissolved organic matter in the ocean, Nature, 386, 480-482, doi: 10.1038/386480a0, 1997.

Opsahl, S. and Benner, R.: Photochemical reactivity of dissolved lignin in river and ocean waters, Limnology and Oceanography, 43, 1297-1304, doi: 10.4319/lo.1998.43.6.1297, 1998.

Osterholz, H., Kirchman, D. L., Niggemann, J., and Dittmar, T.: Environmental Drivers of Dissolved Organic Matter Molecular Composition in the Delaware Estuary, Frontiers in Earth Science, 4, doi: 10.3389/feart.2016.00095, 2016.

Peierls, B. L. and Paerl, H. W.: Temperature, organic matter, and the control of bacterioplankton in the Neuse River and Pamlico Sound estuarine system, Aquatic Microbial Ecology, 60, 139-149, doi: 10.3354/ame1415, 2010.

Polimene, L., Pinardi, N., Zavatarelli, M., Allen, J. I., Giani, M., and Vichi, M.: A numerical simulation study of dissolved organic carbon accumulation in the northern Adriatic Sea, Journal of Geophysical Research, 112, doi: 10.1029/2006jc003529,

2007.

Qi, J., Chen, C., Beardsley, R. C., Perrie, W., Cowles, G. W., and Lai, Z.: An unstructured-grid finite-volume surface wave model (FVCOM-SWAVE): Implementation, validations and applications, Ocean Modelling, 28, 153-166, doi: 10.1016/j.ocemod.2009.01.007, 2009.

Raymond, P. A. and Bauer, J. E.: Use of ^{14}C and ^{13}C natural abundances for evaluating riverine, estuarine, and coastal DOC and POC sources and cycling: a review and synthesis, Organic Geochemistry, 32, 469-485, doi: 10.1016/s0146-6380(00)00190-x, 2001.

Romera-Castillo, C., Sarmento, H., Alvarez-Salgado, X. A., Gasol, J. M., Marrasé, C. J. A., and microbiology, e.: Net production and consumption of fluorescent colored dissolved organic matter by natural bacterial assemblages growing on marine phytoplankton exudates, 77, 7490-7498, 2011.

Sanches, L. F., Guenet, B., Marino, N. d. A. C., and de Assis Esteves, F.: Exploring the drivers controlling the priming effect and its magnitude in aquatic systems, Journal of Geophysical Research: Biogeosciences, 126, e2020JG006201, doi: 10.1029/2020JG006201, 2021.

Shang, R., Wang, Z., Zhang, C., and Shi, X.: Distribution of dissolved organic carbon in the Yellow Sea and East China Sea in winter, Advances in Marine Science, 30, 94-101, doi: 10.1007/s11783-011-0280-z, 2012.

Shen, Y. and Benner, R.: Mixing it up in the ocean carbon cycle and the removal of refractory dissolved organic carbon, Scientific Reports, 8, doi: 10.1038/s41598-018-20857-5, 2018.

Shen, Y., Fichot, C. G., Liang, S.-K., and Benner, R.: Biological hot spots and the accumulation of marine dissolved organic matter in a highly productive ocean margin, Limnology and Oceanography, 61, 1287-1300, doi: 10.1002/lno.10290, 2016.

Shi, G., Peng, C., Wang, M., Shi, S., Yang, Y., Chu, J., Zhang, J., Lin, G., Shen, Y., and Zhu, Q.: The spatial and temporal distribution of dissolved organic carbon exported from three Chinese rivers to the China Sea, Plos One, 11, doi: 10.1371/journal.pone.0165039, 2016.

Shi, X., Li, H., and Zhang, C.: Distribution of dissolved organic carbon in the Yellow Sea and the East China Sea in summer, 2006, Advances in Marine Science, 31, 391-397, doi: 10.1109/ICEICE.2012.655, 2013.

Sokoletsky, L., Yang, X., and Shen, F.: MODIS-based retrieval of suspended sediment concentration and diffuse attenuation coefficient in Chinese estuarine and coastal waters, Conference on Ocean Remote Sensing and Monitoring from Space, Beijing, CHINA, 10.1117/12.2069205, 2014.

Søndergaard, M., Stedmon, C. A., and Borch, N. H.: Fate of terrigenous dissolved organic matter (DOM) in estuaries: Aggregation and bioavailability, Ophelia, 57, 161-176, doi: 10.1080/00785236.2003.10409512, 2003.

Song, S., Gao, L., Li, D., Wang, T., Zhu, L., and Liu, Y.: Distributions and dynamics of dissolved carbohydrate species in Changjiang Estuary and the adjacent East China Sea, Marine Chemistry, 194, 22-32, doi: 10.1016/j.marchem.2017.04.002, 2017.

Sun, X., Li, P., Zhou, Y., He, C., Cao, F., Wang, Y., Shi, Q., and He, D.: Linkages Between Optical and Molecular Signatures of Dissolved Organic Matter Along the Yangtze River Estuary-to-East China Sea Continuum, Frontiers in Marine Science, 9,

36

doi: 10.3389/fmars.2022.933561, 2022.

Tian, D., Zhou, F., Zhang, W., Zhang, H., Ma, X., and Guo, X.: Effects of dissolved oxygen and nutrients from the Kuroshio on hypoxia off the Changjiang River estuary, Journal of Oceanology and Limnology, 40, 515-529, doi: 10.1007/s00343-021-0440-3, 2021.

780   Verhoeven, J. T. A. and Liefveld, W. M.: The ecological significance of organochemical compounds in Sphagnum, Acta Botanica Neerlandica, 46, 117-130, 1997.

Vilge-Ritter, A., Masion, A., Boulange, T., Rybacki, D., and Bottero, J. Y.: Removal of natural organic matter by coagulation-flocculation: A pyrolysis-GC-MS study, Environmental Science & Technology, 33, 3027-3032, doi: 10.1021/es981232p, 1999.

785   Wang, T., Liu, G., and Zhu, L.: Distribution and controlling factors of the dissolved organic carbon in the adjacent sea area of the Yangtze Estuary in winter and summer, Marine Science Bulletin, 33, 533-540, 2014.

Wang, X., Chen, R. F., and Gardner, G. B.: Sources and transport of dissolved and particulate organic carbon in the Mississippi River estuary and adjacent coastal waters of the northern Gulf of Mexico, Marine Chemistry, 89, 241-256, doi: 10.1016/j.marchem.2004.02.014, 2004.

790   Wang, X., Ma, H., Li, R., Song, Z., and Wu, J.: Seasonal fluxes and source variation of organic carbon transported by two major Chinese Rivers: The Yellow River and Changjiang (Yangtze) River, Global Biogeochemical Cycles, 26, doi: 10.1029/2011GB004130, 2012.

Wang, Y., Shen, J., and He, Q.: A numerical model study of the transport timescale and change of estuarine circulation due to waterway constructions in the Changjiang Estuary, China, Journal of Marine Systems, 82, 154-170, doi:
795   https://doi.org/10.1016/j.jmarsys.2010.04.012, 2010.

Wetz, M. S. and Yoskowitz, D. W.: An 'extreme' future for estuaries? Effects of extreme climatic events on estuarine water quality and ecology, Marine Pollution Bulletin, 69, 7-18, doi: 10.1016/j.marpolbul.2013.01.020, 2013.

Wu, L., Chen, C., Guo, P., Shi, M., Qi, J., and Ge, J.: A FVCOM-based unstructured grid wave, current, sediment transport model, I. Model description and validation, Journal of Ocean University of China, 10, 1-8, doi: 10.1007/s11802-011-1788-3,
800   2011.

Xing, J., Xian, W., and Sheng, X.: Distribution characteristics of dissolved organic carbon and influence factors in the Yangtze River Estuary during 2012, Periodical of Ocean University of China, 44, 74-82, doi: 10.16441/j.cnki.hdxb.2014.08.011, 2014.

Yang, S., Han, X., Zhang, C., Sun, B., Wang, X., and Shi, X.: Seasonal changes in phytoplankton biomass and dominant
805   species in the Changjiang River Estuary and adjacent seas: General trends based on field survey data 1959–2009, Journal of Ocean University of China, 13, 926-934, doi: 10.1007/s11802-014-2515-7, 2014.

Yang, S. L., Xu, K. H., Milliman, J. D., Yang, H. F., and Wu, C. S.: Decline of Yangtze River water and sediment discharge: Impact from natural and anthropogenic changes, Scientific Reports, 5, 12581, doi: 10.1038/srep12581, 2015.

Yuan, H., Song, J., Li, X., Li, N., Duan, L., Qu, B., Lu, X., and Chen, X.: Distribution and impact factors of dissolved

37

organic carbon in the Southern Yellow Sea and the Changjiang Estuary in summer, Journal of Guangxi Academy of Science, 31, 155-160, doi: 10.13657/j.cnki.gxkxyxb.20150819.006, 2015.

Zhang, L., Xue, M., Wang, M., Cai, W., Wang, L., and Yu, Z.: The spatiotemporal distribution of dissolved inorganic and organic carbon in the main stem of the Changjiang (Yangtze) River and the effect of the Three Gorges Reservoir, Journal of Geophysical Research: Biogeosciences, 119, 741-757, doi: 10.1002/2012jg002230, 2014.

Zhang, S., Xian, W., and Liang, C.: Distribution characteristics of total organic carbon and influence factors in the Yangtze River Estuary in autumn 2015, Marine Environmental Science, doi: 10.13634/j.cnki.mes.2018.01.010, 2018.

Zhang, S., Wang, J., Li, N., and Yan, X.: Dissolved organic carbon and nitrogen in Changjiang Estuary and adjacent sea areas in spring, Marine Environmental Science, 32, 33-37, 2013.

Zhang, T., Wang, Z., Shi, X., and Zhang, C.: Spatial distribution of dissolved organic carbon in the Yellow Sea and East China Sea, Marine Environmental Science, 30, doi: 10.3969/j.issn.1007-6336.2011.02.003, 2011.

Zhang, W., Xu, Y. J., Guo, L., Lam, N. S. N., Xu, K., Yang, S., Yao, Q., and Liu, K.-b.: Comparing the Yangtze and Mississippi River Deltas in the light of coupled natural-human dynamics: Lessons learned and implications for management, Geomorphology, 399, 108075, doi: 10.1016/j.geomorph.2021.108075, 2022.

Zhang, Y., Ren, J., Zhang, W., and Wu, J.: Importance of salinity-induced stratification on flocculation in tidal estuaries, Journal of Hydrology, 596, doi: 10.1016/j.jhydrol.2021.126063, 2021.

Zhao, C., Hou, Y., Wang, Y., Li, P., He, C., Shi, Q., Yi, Y., and He, D.: Unraveling the photochemical reactivity of dissolved organic matter in the Yangtze river estuary: Integrating incubations with field observations, Water Research, 245, doi: 10.1016/j.watres.2023.120638, 2023.

Zheng, L., Chen, B., Liu, X., Huang, B., Liu, H., and Song, S.: Seasonal variations in the effect of microzooplankton grazing on phytoplankton in the East China Sea, Continental Shelf Research, 111, 304-315, doi: 10.1016/j.csr.2015.08.010, 2015.

Zhu, Z.-Y., Ng, W.-M., Liu, S.-M., Zhang, J., Chen, J.-C., and Wu, Y.: Estuarine phytoplankton dynamics and shift of limiting factors: A study in the Changjiang (Yangtze River) Estuary and adjacent area, Estuarine, Coastal and Shelf Science, 84, 393-401, doi: 10.1016/j.ecss.2009.07.005, 2009.